EMPIRICAL SCALING OF STRONG EARTHQUAKE GROUND MOTION - PART I: ATTENUATION AND SCALING OF RESPONSE SPECTRA

V.W. Lee

Civil Engineering Department
University of Southern California
Los Angeles, California, U.S.A.

ABSTRACT

Three generations of empirical scaling equations, developed by the Strong Motion Research Group at University of Southern California in the 1970's, 1980's and 1990's, for the attenuation and scaling of spectral amplitudes of strong ground motion are reviewed. Semi-theoretical extrapolation functions for extending these empirical scaling equations to high and low frequencies are also presented. For brevity, only equations and illustrations which describe the relative response spectrum amplitudes are shown, but the methods and procedures presented are also applicable to scaling of Fourier amplitude spectra, for which complete corresponding references are also included.

KEYWORDS: PSV, Attenuation, Earthquake Source, Path Type, Local Geology and Soil

INTRODUCTION

In this paper, a review of selected scaling methods for the estimation of spectral amplitudes of strong earthquake ground motion will be presented. Since late 1960's, this work has advanced so much that at present, very detailed scaling equations are available for empirical estimation of strong motion amplitudes in California. For studies dealing with source mechanism and prediction of synthetic strong ground motion, the Fourier amplitude spectra are required (e.g., Lee and Trifunac, 1993; Trifunac, 1973, 1976b, 1989a, 1989b, 1989c, 1991a, 1993a; Trifunac and Lee, 1978, 1980, 1989a). For engineering estimation of the response of structures, several forms of relative response spectra are used (Trifunac, 1977a, 1977b, 1991a, 1994e; Trifunac and Anderson, 1978a, 1978b, 1978c; Trifunac and Gupta, 1991; Trifunac and Lee, 1989b). For simplicity and brevity in the following, empirical scaling of pseudo relative velocity (PSV) spectrum only will be described. *Mutatis mutandis* most of the methods will be applicable also for the scaling of Fourier spectrum amplitudes.

This paper is divided into four parts. The first part reviews the first generation of direct scaling equations of PSV amplitudes, and is based on the paper by Trifunac (1978). The second part introduces frequency-dependent attenuation equations and dependence of the direct scaling equations on local soil and local geologic site conditions. It also presents two parallel approaches, one based on magnitude and the other on intensity scale. This part is based on the papers by Trifunac and Lee (1985a, 1985b, 1985c, 1987). In the third part, direct scaling equations for PSV amplitudes which have been refined during the early 1990's and the new scaling models, as described in the reports by Lee and Trifunac (1995a, 1995b), are presented. Finally in the fourth part, the methods for extrapolation of spectral amplitudes to long $(T > 10 \text{ s})$ and short $(T < 0.04 \text{ s})$ periods (Trifunac, 1993a, 1993b, 1994a, 1994b, 1994c, 1994d, 1995a, 1995b) will be summarized.

The concept of response spectrum was introduced into earthquake engineering by Biot (1932, 1933, 1934, 1941, 1942) and Benioff (1934). Following the gradual accumulation of strong motion recordings since 1934, the response spectrum method for the design of earthquake-resistant structures (Hudson et al., 1972) is now a part of or is being introduced into many modern earthquake design codes (Newmark et al., 1977).

There are difficulties which result from the oversimplified methodology associated with the common response spectrum approach. Some are caused by the lack of information contained in the response spectrum or result from its definition, which is the maximum amplitude of the entire time-history response to ground motion. Many details on the duration of strong shaking (Trifunac and Brady, 1975a; Trifunac and Novikova, 1994) and on the number and the distribution of peak amplitudes in the response

are essentially eliminated (Gupta and Trifunac, 1988a, 1990a, 1990b, 1991a, 1991b). Other problems occur because the response analysis is linear. This makes the estimates of more realistic non-linear response difficult. In a non-linear progressively deteriorating structural system, strong shaking with same peak amplitudes may result in no damage, partial damage or total damage, depending on whether a structure was strained through one, several or many cycles of non-linear response. In spite of these and other well-known difficulties, the simplified response spectrum approach has gained considerable popularity among the engineering profession. If used judiciously and with awareness of its limitations, it may offer convenient and simple means for the design of earthquake-resistant structures.

The physical phenomena which cause strong shaking are described by parameters related to the earthquake source mechanism (seismic moment, fault geometry, dislocation amplitudes, stress drop, radiation pattern, etc.) and the transmission path. For engineering analyses, however, at present one still has to use less sophisticated parameters to describe strong shaking; e.g., earthquake magnitude (Trifunac, 1991b), epicentral distance, site conditions, Modified Mercalli Intensity (Trifunac, 1977c; Trifunac and Todorovska, 1989a, 1989b; Trifunac and Zivčić, 1991; Trifunac et al., 1988, 1991; Trifunac and Brady, 1975b, 1975c; Wong and Trifunac, 1979). This is because those simple parameters are readily available and can be processed to yield desired statistical or deterministic estimates of future earthquake shaking.

Different types of response spectra are calculated from strong-motion accelerograms (Hudson et al., 1972). In this paper, we begin by reviewing briefly the absolute acceleration spectrum, SA, which represents the maximum absolute acceleration of a single-degree-of-freedom system, with prescribed fraction of critical damping, during the excitation by a strong-motion accelerogram. The scaling of the absolute acceleration spectra, SA, can be considered in terms of two groups of parameters. The first group will consist of earthquake magnitude, M, epicentral distance, R, recording site conditions, s ($s = 0$ will be assigned to alluvium sites, $s = 2$ to hard basement rock sites, and $s = 1$ to intermediate sites; see Trifunac (1990a)), component direction ($v = 0$ for horizontal, and $v = 1$ for vertical motion), and a parameter, p, which will describe approximately the distribution of the spectral amplitudes. The second group will consist of the Modified Mercalli Intensity (MMI) in place of M, and the epicentral distance, R, will be deliberately omitted to avoid explicit emphasis on the rate of attenuation of MMI in California. While this omission will increase the scatter of the observed spectral amplitudes with respect to the assumed empirical model, it will permit the use of the derived correlations outside California, at least formally.

Following the first recordings of strong ground motion in 1934, 1940 and 1952, and the early systematic calculations of response spectrum amplitudes (Alford et al., 1951), it became possible to study the shape of response spectra. This led to the early development of "standard" spectral shapes for use in design. This concept was first proposed by Biot (1942) and carried out in the late 1950's (Housner, 1970), and extends to the present through cycles driven by the availability of new data. The early work was usually characterized by the fixed shape of response spectrum whose amplitude depended on a single scaling parameter. Though spectra were also developed (Veletsos et al., 1965) for scaling in terms of peak acceleration, peak velocity and peak displacement, the direct availability of peak acceleration amplitudes from recorded accelerograms and the lack of accurate and uniformly processed peak velocities and peak displacements (Trifunac, 1976a, 1976c) meant that most of the design spectra were essentially scaled by the peak acceleration alone (Trifunac and Brady, 1975d, 1975e; Trifunac and Lee, 1992). It was recognized that the shape of response spectra should depend on such parameters as earthquake magnitude, and source-to-station distance, but the data available in the mid- and late 1950's did not allow more refined analyses.

With the availability of additional strong motion recordings in the mid 1960's and early 1970's, it became possible to improve upon these early studies. One example of such an improved set of fixed shape absolute acceleration spectra was developed for the design of nuclear power plants (Nuclear Regulatory Commission Guide 1.60 spectra; see Newmark et al. (1973), Trifunac and Anderson (1977)). These spectra were still scaled by peak acceleration amplitudes, and the effects of magnitude, source-to-station distance, attenuation with distance and site conditions were introduced only through the modification of peak acceleration.

Observed damage from earthquake shaking depends on the geologic and local soil conditions. Numerous attempts have been made to relate this observation to the recorded strong-motion accelerations (Duke, 1958), and to the recordings on more sensitive seismological instruments (Gutenberg, 1957;

Borcherdt and Gibbs, 1976). With the exception of the work by Gutenberg (1957), most studies dealing with these effects attempted to relate the variations in damage to peak accelerations or peak velocity only, and thus explicitly or implicitly ignored the frequency-dependent nature of this problem.

Seed et al. (1974) presented one of the firs6t studies of the frequency-dependent variations of spectrum shape. In their analysis, the dependence of the spectral amplitudes on site conditions was investigated by carrying out four independent statistical analyses. The explicit dependence of spectrum shapes on magnitude and source-to-station distance were eliminated, however, by normalization of all spectral amplitudes to peak acceleration.

After the completion of the first phase of the uniform data processing effort (Trifunac, 1977d), it became possible to develop first multi-dimensional regression analyses of the shape and amplitudes of response spectra, as those depend not only on the recording site conditions, but also on other important parameters describing the strong ground motion. The first and pioneering studies on how the Fourier amplitude spectra depend on such scaling parameters (Trifunac, 1976b), have shown that similar correlations for absolute acceleration and other response spectra will produce equally valuable results.

FIRST DIRECT SCALING EQUATIONS FOR PSEUDO RELATIVE VELOCITY

The experience gained from the first direct scaling of the Fourier amplitude spectra (Trifunac, 1976b) and later of absolute acceleration spectra (Trifunac and Anderson, 1977) was next applied to direct scaling of PSV spectra. The database for this analysis resulted from recordings of 57 earthquakes whose magnitudes ranged from 3.0 to 7.7. Sixty-three percent of this data has been recorded on alluvium sites, 23% on "intermediate sites", and only 8% on basement rock sites. This site classification was proposed by Trifunac (see Trifunac and Brady (1975b)) to characterize roughly the geologic environment of the recording station. It has been designed for use with geologic maps, and for alluvium and sedimentary deposits with depths measured in thousands of feet (not hundreds of feet). For geological site characterization, ideally a site should be classified either as alluvium site $(s = 0)$ or as basement rock site $(s = 2)$. However, recognizing that in some cases, it may be difficult to make a choice in a complex geologic environment or that insufficient or no data are available on site characteristics, "intermediate" $(s = 1)$ site classification has been introduced and assigned to 23% of 187 records.

1. Direct Scaling of PSV Spectra in Terms of Magnitude and Source-to-Station Distance

For scaling of PSV spectra in terms of magnitude M, epicentral distance R, recording site conditions s, component direction v, and a parameter, p, which approximately determines the fraction of spectral amplitudes smaller than the selected spectra $\text{PSV}(T),_p$, we employed (Trifunac, 1978)

$$\log[\text{PSV}(T),_p] = M + \log A_0(R) - a(T)p - b(T)M - c(T) - d(T)s - e(T)v - f(T)M^2 - g(T)R \quad (1)$$

The functional form of Equation (1) has been motivated by the pioneering work of Trifuanc (1976b) and by the definition of local magnitude scale which states that the logarithm of peak amplitude on a standard instrument corrected for distance attenuation $[\log A_0(R)]$ is equal to the magnitude (Richter, 1958; Trifunac, 1991b). The terms $a(T)p + b(T)M + c(T) + d(T)s + e(T)v + f(T)M^2 + g(T)R$ then represent an empirical correction that depends on $M, p, s, v,$ and R. The term $a(T)p$, in which p is not probability, but a parameter related to probability of exceedance (Trifunac and Anderson, 1978a), approximates the distribution of observed amplitudes of $\text{PSV}(T)$ about Equation (1) when $0.1 \le p \le 0.9$. The terms $b(T)M$ and $f(T)M^2$ model the diminishing growth of spectral amplitudes with increasing magnitude (Trifunac, 1973, 1976a, 1976b). Functions $d(T)$ and $e(T)$ model the frequency-dependent differences in spectral amplitudes for: (1) alluvium relative to basement rock sites; and (2) horizontal relative to vertical ground motion. Anelastic and scattering attenuation of amplitude with distance is often described by $\exp(-\pi R/(TQ\beta))$, where Q is the quality factor of the medium and β is the shear wave velocity (Trifunac, 1994b). The physical meaning of $g(T)$ in Equation (1) is then that it corresponds to $(\pi/TQ\beta) \times \log e$.
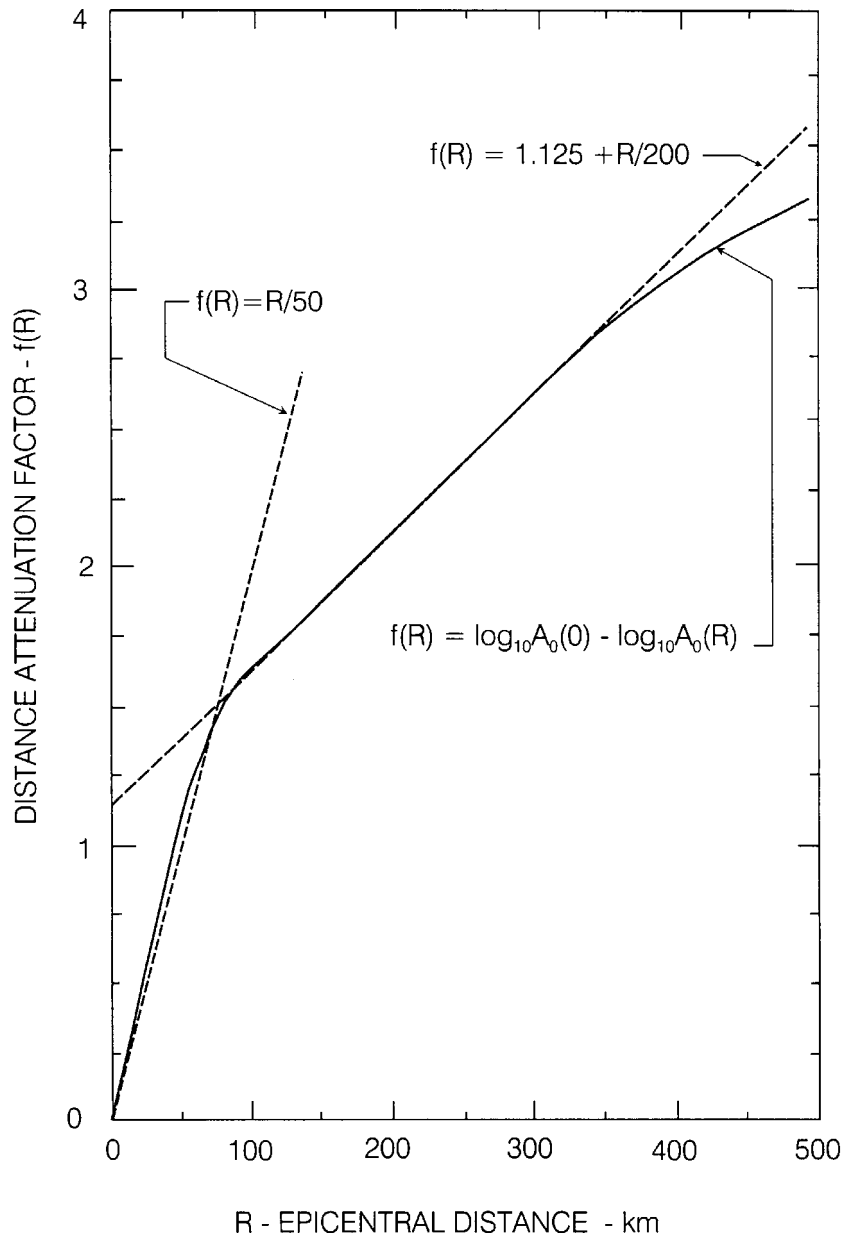
Fig. 1 Distance attenuation factor $f(R)$

The amplitude attenuation with distance has been modeled by the term $\log A_0(R)$. Figure 1 presents the plot of $f(R)$ defined so that

$$\log A_0(R) = \log A_0(R = 0) - f(R) \qquad (2)$$

and shows that $f(R)$ can be approximated by $R/50$ for $R \leq 75\,\text{km}$ and by $1.125 + R/200$ for $350 \geq R \geq 75\,\text{km}$.

The change in slope at $R = 75$ km results from slower attenuation of surface waves with distance $\left(\sim 1/R^{1/2} \right)$, from the fact that in this distance range, surface waves emerge as the main contributors to strong shaking, and from strong reflections off the Moho discontinuity. The near- and intermediate-field terms of strong motion amplitudes attenuate like $1/R^4$ to $1/R^2$, while the amplitudes of body waves diminish as $1/R$. Thus, $f(R)$ [i.e., $\log A_0(R)$] represents an empirical description of how strong motion amplitudes decay with distance. The fact that $\log A_0(R)$ results from observations of actual wave attenuation with distance in California, suggests that this description of the changes of strong motion amplitudes with distance may be easier to justify on physical grounds than the frequently used

expressions of the form $(R+a)^{-n}$, in which a is some constant. There are several obvious disadvantages in using $(R+a)^{-n}$. First, for $R << a$, it tends to a constant a^{-n} for all frequencies of motion. This may lead to difficulties in modeling the near-field terms that attenuate like $1/R^2$ and $1/R^4$. Secondly, $(R+a)^{-n}$ experiences a rapid change of slope near $R=a$, from zero to $-n$. Finally, for $R >> a$, the values of n usually between 1 and 2 lead to too rapid amplitude attenuation with distance that is incompatible with surface wave attenuation (Trifunac and Lee, 1985a, 1990; Lee and Trifunac, 1995a).
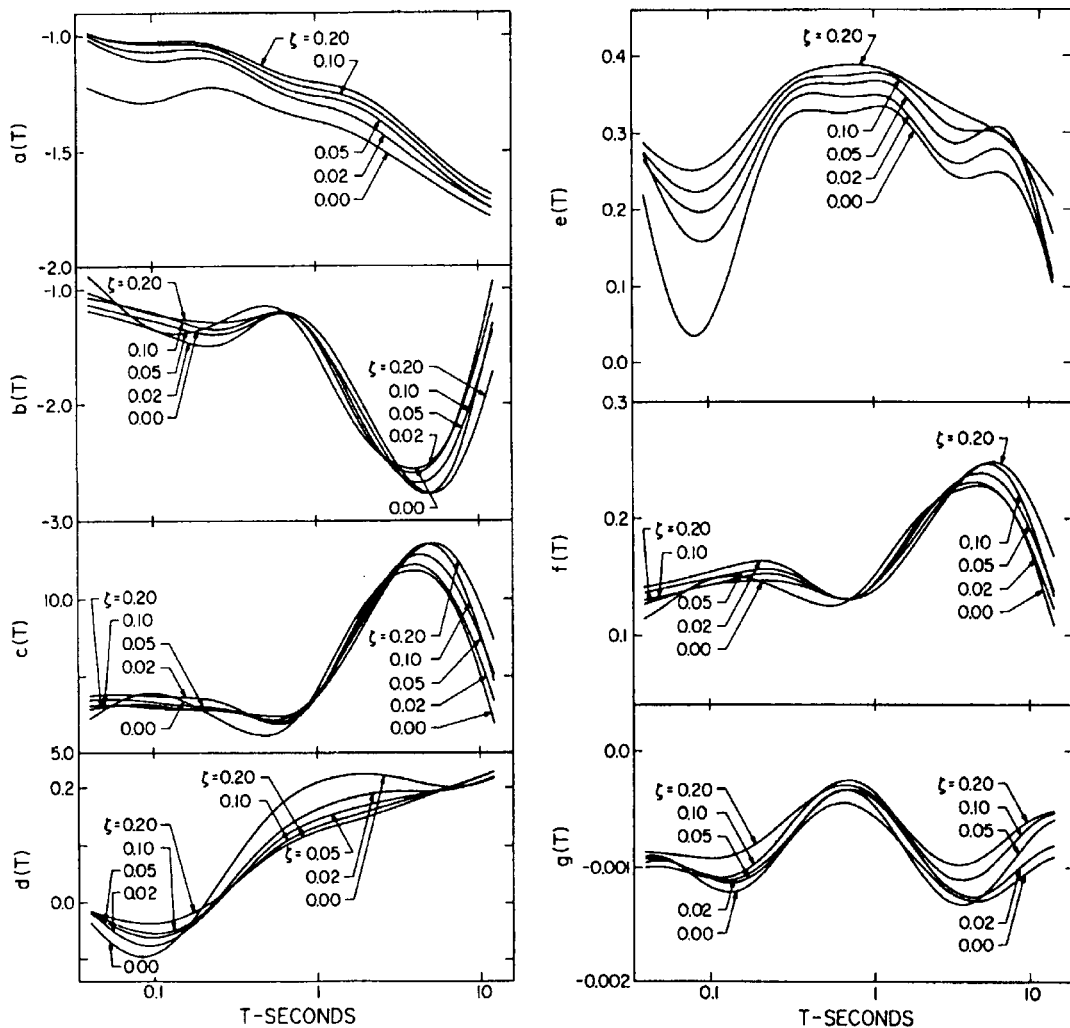
Fig. 2 Functions $a(T), b(T),...f(T)$ and $g(T)$

To compute the coefficient functions $a(T), b(T), ...$, Trifunac (1978) partitioned all data into four groups corresponding to the magnitude ranges $4.0-4.9, 5.0-5.9, 6.0-6.9,$ and $7.0-7.9$. Each of these groups was next sub-divided into three sub-groups corresponding to the site classification, s. Depending on whether the recording component is horizontal or vertical, each of these sub-groups was finally divided into two parts corresponding to $v=0$ and 1. Within each of these parts, n data points with amplitudes equal to $\log[\text{PSV}(T)] - M - \log A_0(R)$ were arranged so that the numerical values decreased monotonically. Then, if m = integer part of (pn), in which $0.05 \le p \le 0.95$, the $m-$th data point represents an estimate for an upper bound on $\log[\text{PSV}(T)] - M - \log A_0(R),$ so that $100p$ percent of the corresponding data is less than that value. For actual regression calculations, at most 19 values of p equal to 0.05, 0.10, 0.15, ... 0.90 and 0.95 were used. The advantage of this approach was that it eliminated strong dependence of the final regression model on the earthquakes that contributed most to the available data.

Figure 2 presents the amplitudes of $a(T)$, $b(T)$, ... and $g(T)$ for $\zeta = 0.0$, 0.02, 0.05, 0.10, and 0.20 plotted versus T, the undamped period of the single-degree-of-freedom oscillator. Here, ζ represents a fraction of critical damping.

Many features of functions $a(T)$ through $g(T)$ are similar to those found for the scaling of absolute acceleration spectra (Trifunac and Anderson, 1977). The amplitudes of $b(T)$ and $c(T)$, however, differ because of the normalization factors and the units employed in those two analyses, and because $\text{PSV}(T)/\text{SA}(T) \approx T/2\pi$. Figures 3 and 4 present examples of PSV spectra for $R = 0, \zeta = 0.02$, and $p = 0.5$ in Equation (1).
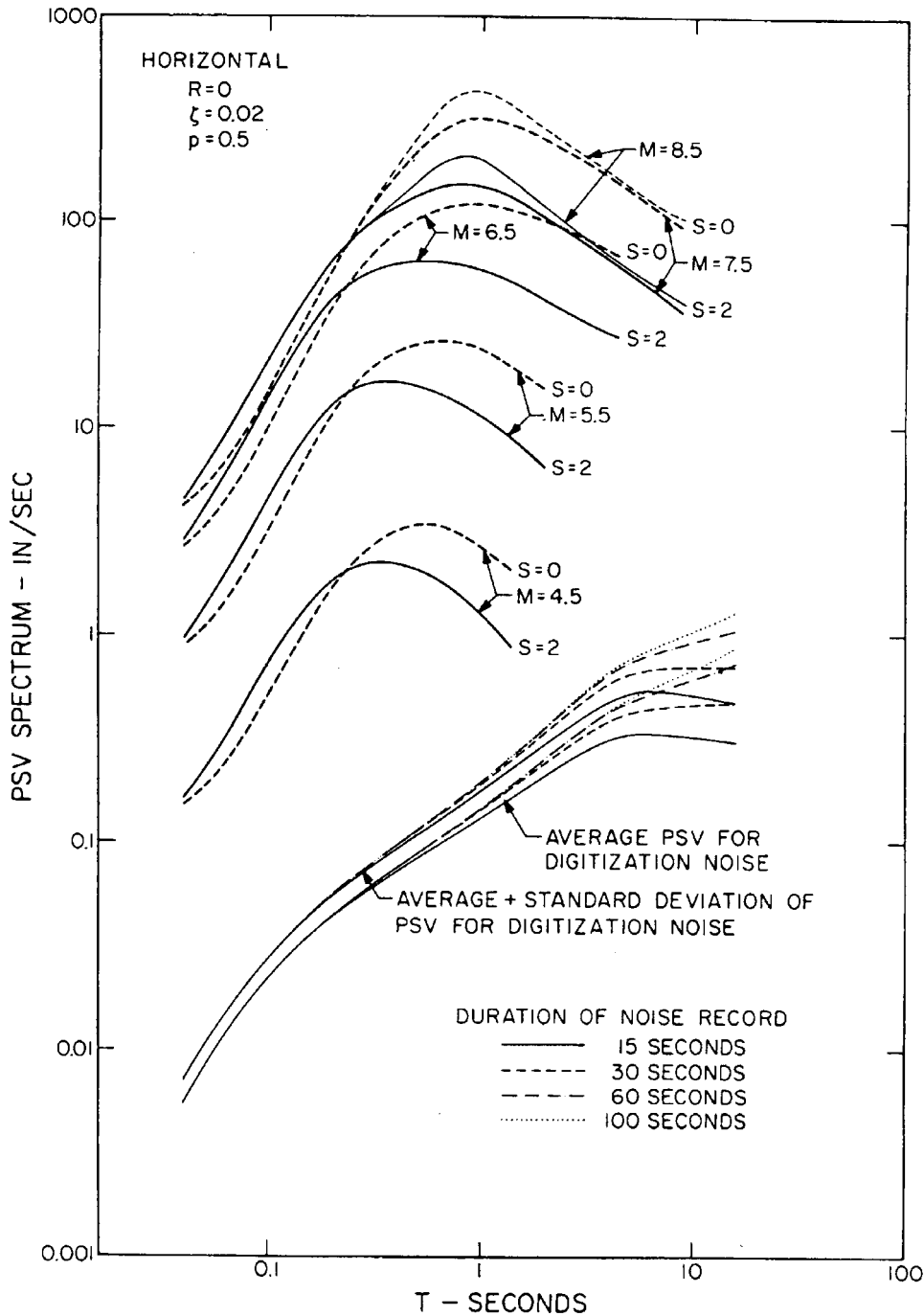
Fig. 3 Horizontal PSV spectra for $M = 4.5$ through 8.5, and for $s = 0$ and 2

The use of Equation (1) is constrained to the interval $M_{\min} \leq M \leq M_{\max}$, in which $M_{\min} = -b(T)/2f(T)$ and $M_{\max} = 1 - b(T)/(2f(T))$. For $M \geq M_{\max}$, M is to be replaced by $M_{\max}$,

and for $M < M_{min}$, M is to be replaced by M_{min}, only in the terms $b(T)M$ and $f(T)M^2$. This leads to linear growth of $\log[\text{PSV}(T)_{,p}]$ with respect to M for $M \leq M_{min}$, to parabolic growth for $M_{min} \leq M \leq M_{max}$, and to constant amplitudes for $M \geq M_{max}$ which are equal to the amplitudes for $M = M_{max}$.
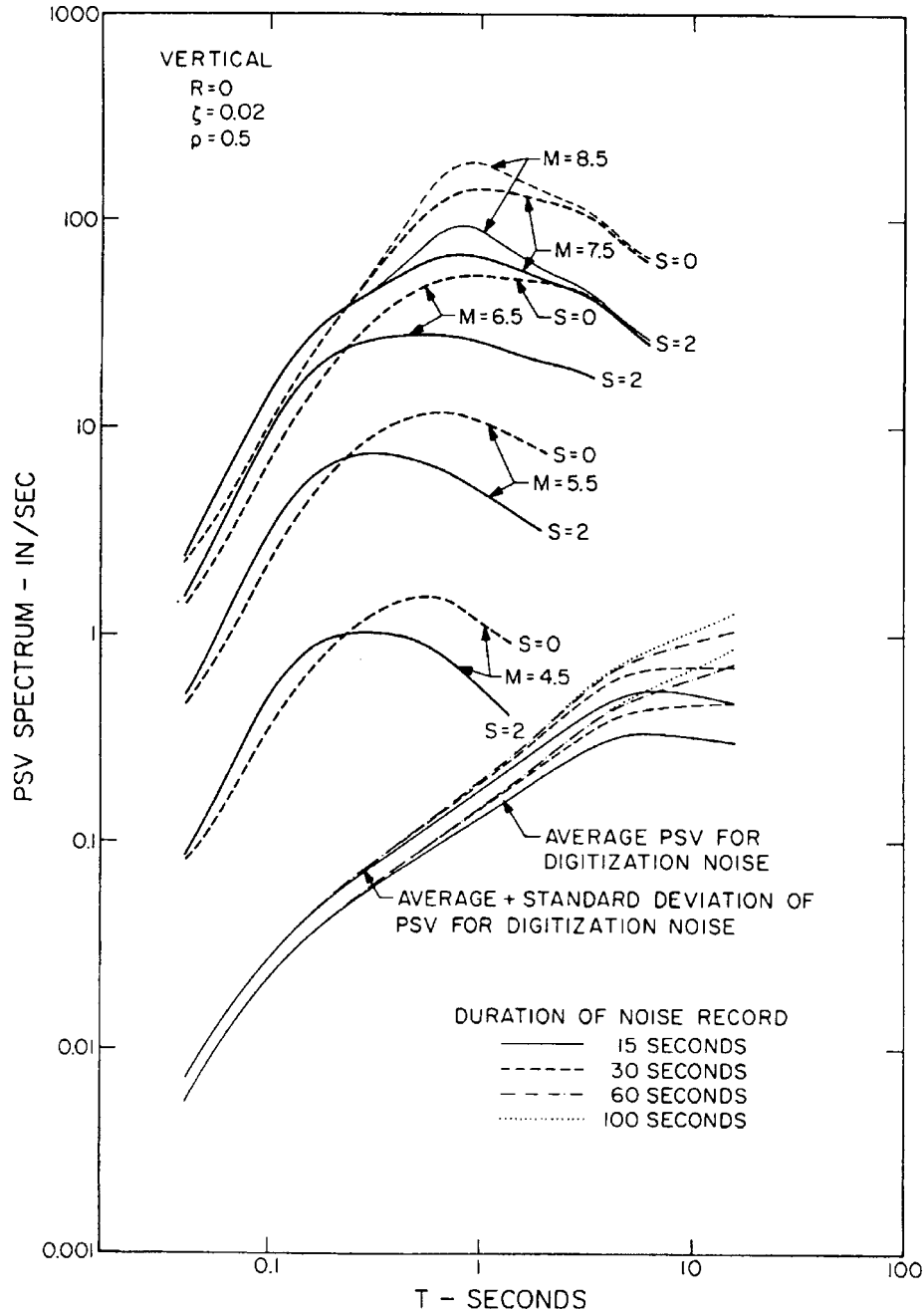
Fig. 4 Vertical PSV spectra for $M = 4.5$ through 8.5, and for $s = 0$ and 2

This type of growth for $\log[\text{PSV}(T)_{,p}]$ with respect to magnitude has been selected to model the effects of diminishing rate of growth of strong motion amplitudes with fault dimensions for large earthquakes with M between about 7.5 and 8.5. Though the precise nature of the growth of spectral amplitudes with M is difficult to decipher from the currently available data, the observations and the spectra of strong shaking so far do not contradict this form of Equation (1). The result of this analysis then is to suggest that the PSV amplitudes essentially cease to grow for $M \approx 7.5$.

Figures 3 and 4 further show the average and average plus one standard deviation of spectral amplitudes for the combined recording and data processing noise (Trifunac and Todorovska, 2001a,

2001b). This noise diminishes the signal-to-noise ratio in many recorded accelerograms for $T > 2$ s and thus the quality of $a(T)$ through $g(T)$ in the same period range. Consequently, the use of Equation (1) is not recommended for periods longer than those for which selected spectral amplitudes have been plotted in Figures 3 and 4.

The shapes of all response spectra should depend on earthquake magnitude, and this dependence is such as to enhance the long period motions for larger magnitudes. Figures 5 and 6 show that this is the case for PSV spectra (normalized to one for $T = 0.04$ s).
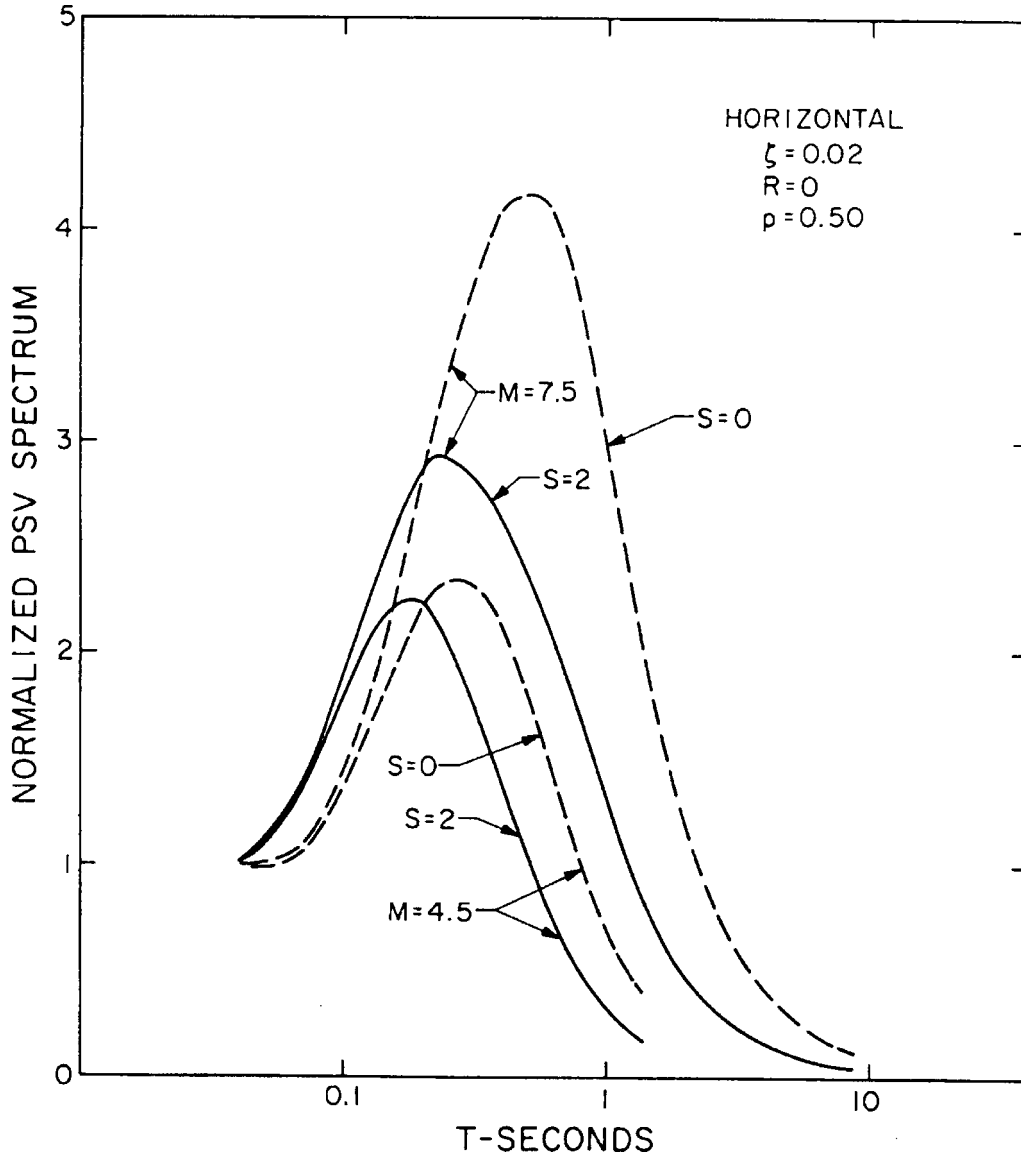
Fig. 5 Change of normalized horizontal PSV spectra with respect to magnitude M and site conditions s

2. Scaling of PSV Spectra in Terms of Modified Mercalli Intensity (MMI)

To scale PSV spectra in terms of MMI, in Equation (1), one can replace M by I_{MM} and delete the terms $\log A_0(R)$ and $g(T)R$ to get (Trifunac, 1979)

$$\log\left[\mathrm{PSV}(T)_{,p}\right] = a(T)p + b(T)I_{MM} + c(T) + d(r)s + e(T)v \tag{3}$$

in which I_{MM} represents discrete levels on MMI scale; p, s, v, and $a(T)$ through $e(T)$ have the same meaning as in Equation (1).
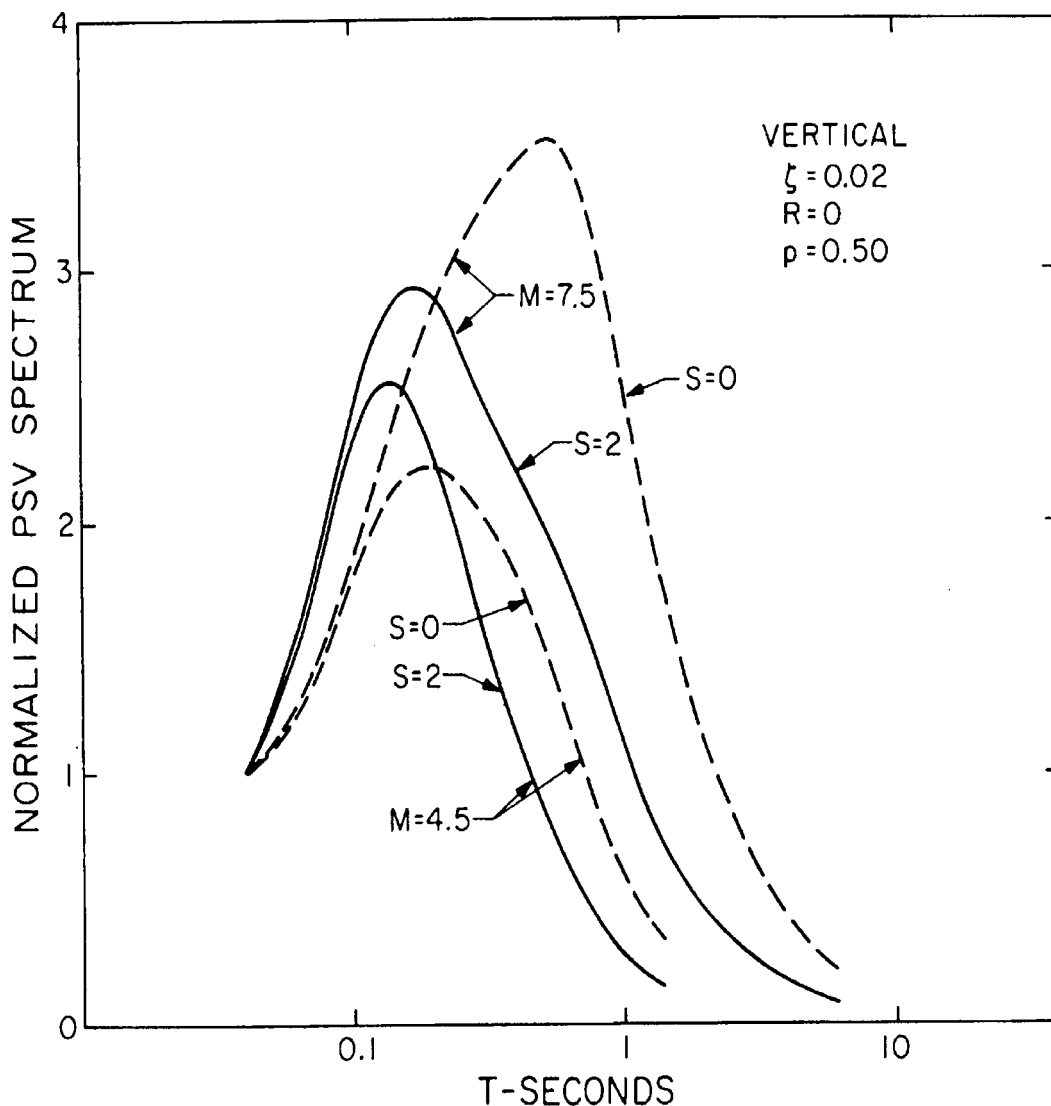
Fig. 6 Change of normalized vertical PSV spectra with respect to magnitude *M* and site conditions *s*

Through the use of regression analysis identical to that which was employed for scaling of absolute acceleration spectra and similar to that described previously for scaling in terms of *M* and *R*, it is possible to compute $a(T)$ through $e(T)$. The results are then as shown in Figure 7 for $\zeta = 0.00, 0.02, 0.05, 0.10,$ and 0.20.

Examples of using Equation (3) for MMI = IV through VIII, for $s = 0$ and 2, for $\zeta = 0.02$ and for $p = 0.5$ are shown in Figure 8 for horizontal and in Figure 9 for vertical PSV spectra. As in Figures 3 and 4, the amplitudes of recording and processing noise are also shown. For the spectra of intensities $MMI \leq VI$, it is seen that the signal-to-noise ratio is small for periods longer than 2-3 s. Consequently, the coefficients $a(T)$ through $e(T)$ in this period range may be affected by this low signal-to-noise ratio, and Equation (3) should not be used in this range. This has been shown in Figures 8 and 9 by terminating spectral amplitudes for MMI = IV and VI at periods shorter than 12 s.

Equation (3) applies to MMI range from IV to VIII only, since it is in this range of intensities that the strong-motion data are currently available. For illustration only, Figures 8 and 9 also show (in light lines) the amplitudes of PSV spectra that result from extrapolating to MMI levels X and XII. By extrapolating to MMI = XII and by comparing the spectral amplitudes with the largest estimates of strong shaking from Equation (1), it is possible to test at least the consistency between the extrapolated maxima computed from Equations (1) and (3). Such a test was performed, and this showed that Equation (3), if extrapolated beyond $I_{MM} = VIII$, yields reasonable estimates of PSV spectral amplitudes for intermediate and low

frequencies. An example of this is presented in Figure 10 where extrapolated PSV spectra (smooth light lines) have been plotted for $\zeta = 0.0, 0.02, 0.05, 0.10,$ and $0.20,$ for $p = 0.1$ and $0.9,$ and for MMI = X and $s = 2,$ the conditions that correspond to the site where the Pacoima Dam accelerogram was recorded during the San Fernando, California, earthquake of 1971.
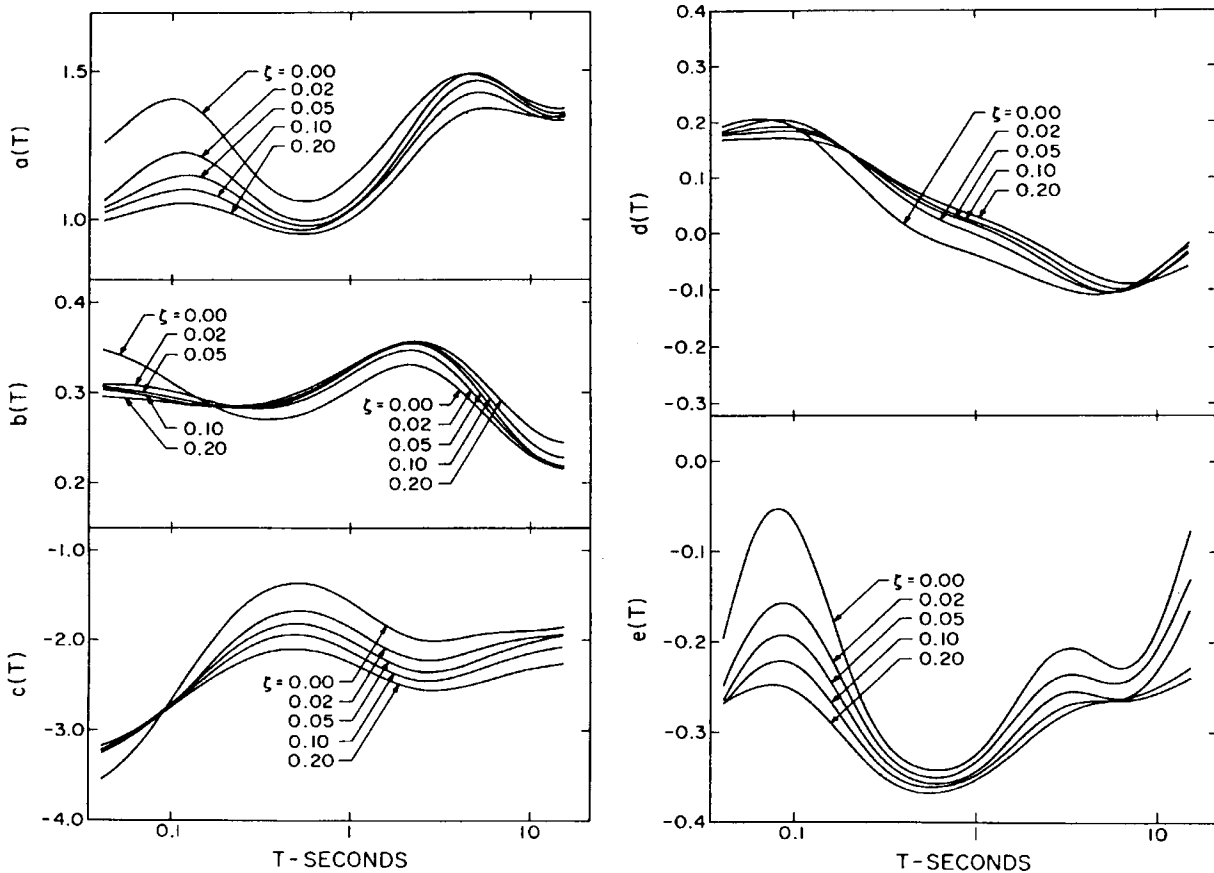
Fig. 7   Functions $a(T), b(T), c(T), d(T)$ and $e(T)$

FREQUENCY-DEPENDENT ATTENUATION AND SIMULTANEOUS TREATMENT OF GEOLOGIC AND SOIL SITE CONDITIONS

The regression analysis of pseudo relative velocity spectra from strong-motion earthquake acceleration records belonging to the first generation of our empirical scaling equations has been outlined in the preceding section (Trifunac, 1978, 1979). There, it was shown that the response spectra of strong motion acceleration can be scaled directly in terms of earthquake magnitude, $M,$ Richter's attenuation function, $A_0(R),$ epicentral distance, $R,$ geological site condition, $s,$ and the component direction, $v,$ without any consideration of peak accelerations. Trifunac and Anderson (1977) used the same scaling function (as for Fourier spectra) to scale absolute acceleration spectra, SA. The same methodology was used to develop analogous functionals for scaling of pseudo relative velocity and relative velocity spectra, PSV and SV (Trifunac and Anderson, 1978a, 1978b). Subsequently, Trifunac and Lee (1979) refined the above analyses by introducing a measure of the depth of sedimentary deposits beneath the recording station, $h,$ as a site characteristic to replace the scaling parameter for site conditions, s. The scaling function then became (Equation (1) of Trifunac and Lee, 1979):

$$\log_{10}\left[\mathrm{PSV}(T)\right] = M + \log_{10} A_0(R) - b(T)M - c(T) - d(T)h - e(T)v - f(T)M^2 - g(T)R \qquad (4)$$

In this equation, $\mathrm{PSV}(T)$ is the PSV amplitude at period $T,$ and $\log_{10} A_0(R)$ represents the empirically determined function, describing the overall attenuation of amplitudes with epicentral distance, R (Richter, 1958). h is the site parameter described above. v is the parameter describing the component

of motion. The scaling functions $b(T)$ through $g(T)$ were determined through the regression analyses at 91 periods, T, between 0.04 s and 15 s.
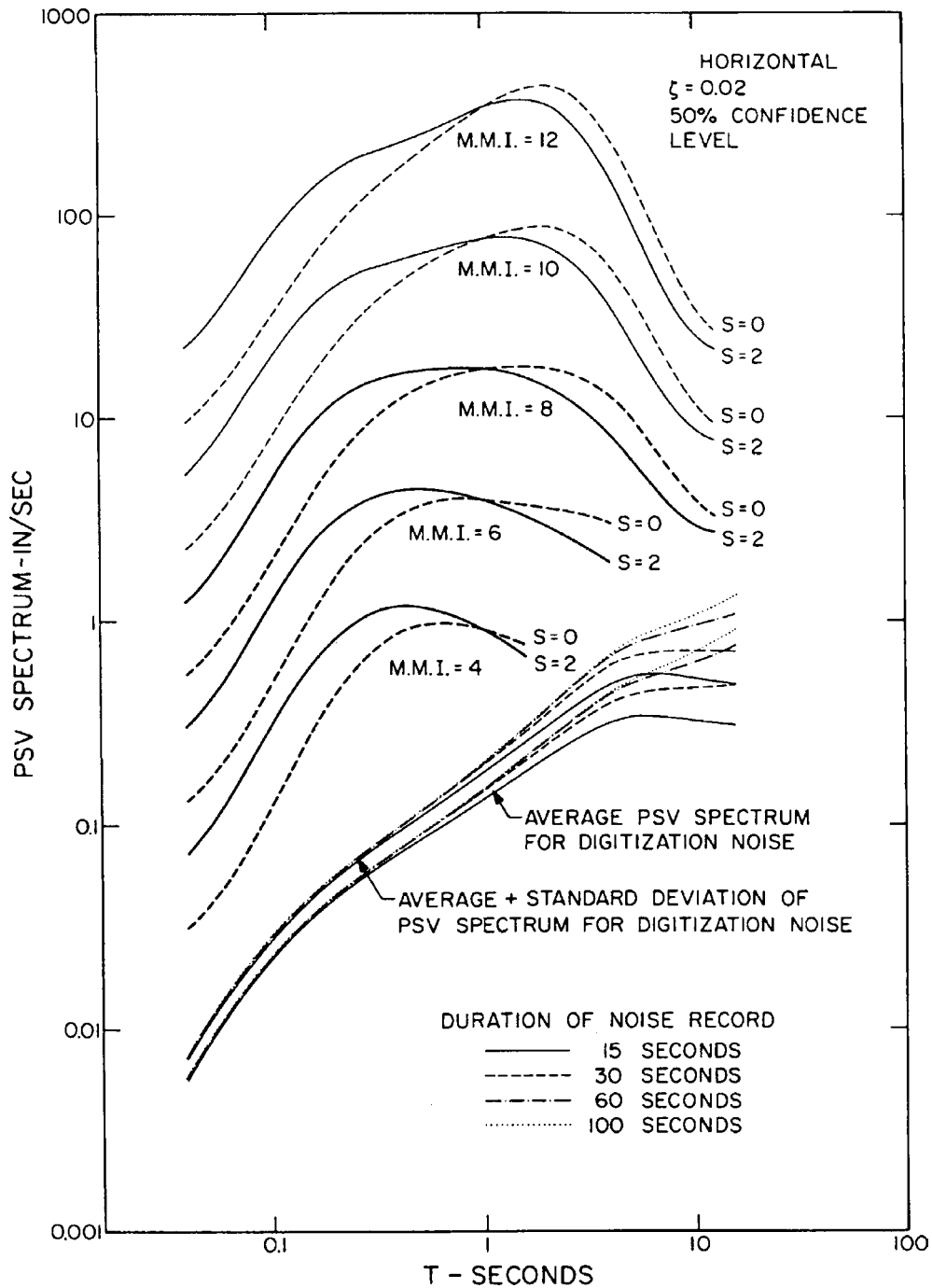
Fig. 8 Horizontal PSV spectra for MMI = IV through XII, and for $s = 0$ and 2

1. Scaling of PSV(*T*) in Terms of *M*, *R*, *H*, *S*, *h* and *v*

1.1 New Regression Analysis (Second Generation of Empirical Scaling Equations)

The first series of regression analyses (during 1970's) of the pseudo relative velocity spectra, PSV(*T*), were carried out for 186 free-field records corresponding to a total of 558 components of data from 57 earthquakes (starting with the Long Beach earthquake in 1933 and ending with the San Fernando earthquake in 1971). The expanded database, which we assembled in early 1980's, consisted of 438 three-component free-field records (1314 components of acceleration) from 104 earthquakes. Most of these earthquakes occurred in the regions of northern and southern California up to the year 1981. With

this new database, Trifunac and Lee (1985a) developed the first frequency-dependent attenuation function, $\text{Att}\left(\Delta, M, T\right)$, as a function of the "representative'" distance Δ from the source to the site, magnitude M and period of the motion T. For a complete description of this attenuation function, the reader is referred to the above reference. Using the same function, Trifunac and Lee (1985b) presented the scaling functions for estimating the Fourier spectral amplitudes, FS(T).
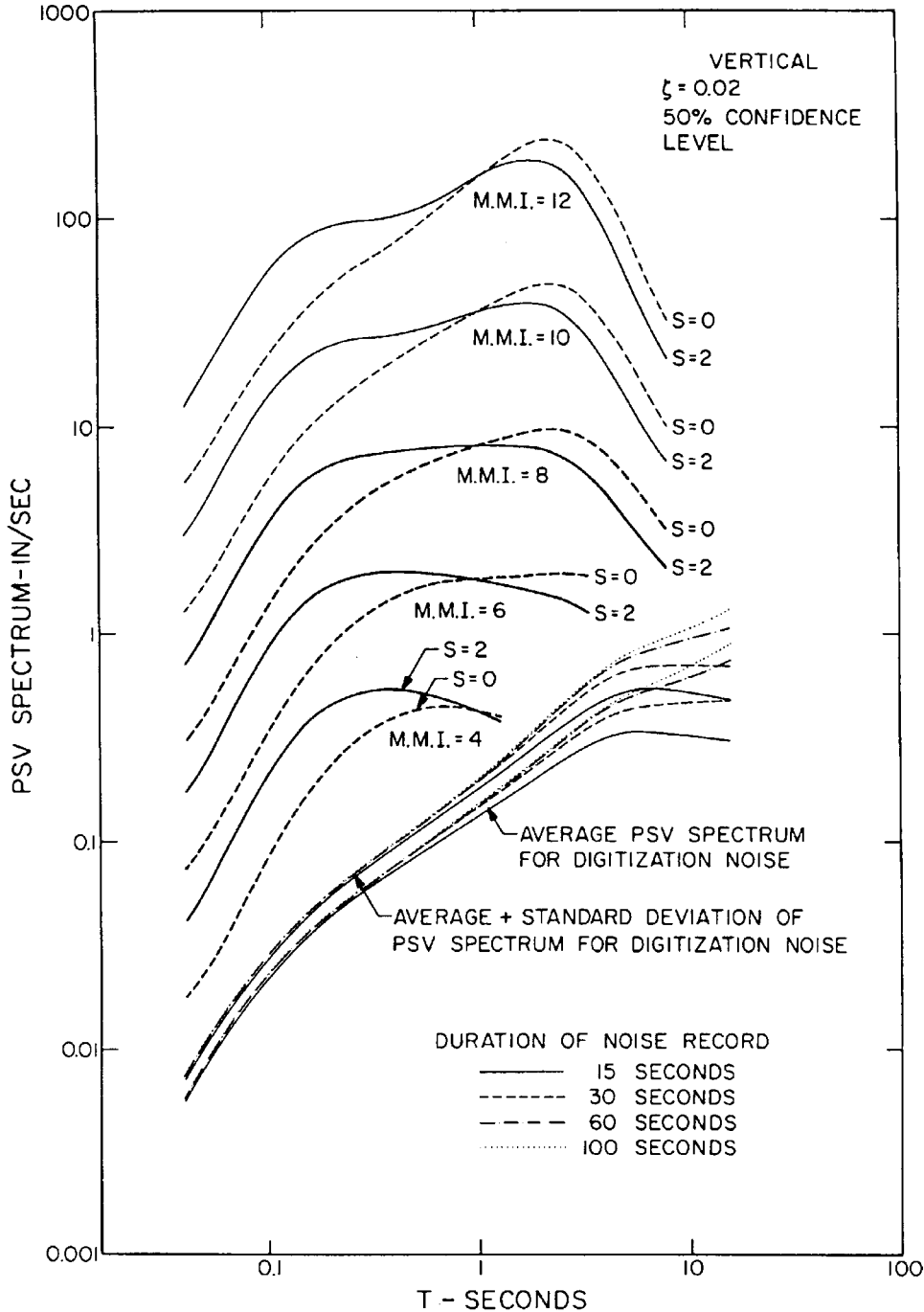
Fig. 9 Vertical PSV spectra for MMI = IV through XII, and for $s = 0$ and 2

Following these new ideas, the dependence of the PSV amplitudes of strong motion at a particular period, T, could be presented in exactly the same form. The scaling equation then became

$$\log_{10}\left[\text{PSV}(T)\right] = M + \text{Att}\left(\Delta, M, T\right) + b_1(T)M + b_2(T)h + b_3(T)v$$
$$+ b_4(T)\Delta/100 + b_5(T) + b_6(T)M^2$$

(5)

Equation (5) is of the same form as in our preceding analyses of spectral amplitudes, but with the old attenuation function $\log_{10} A_0(R)$ replaced by $Att(\Delta, M, T)$.
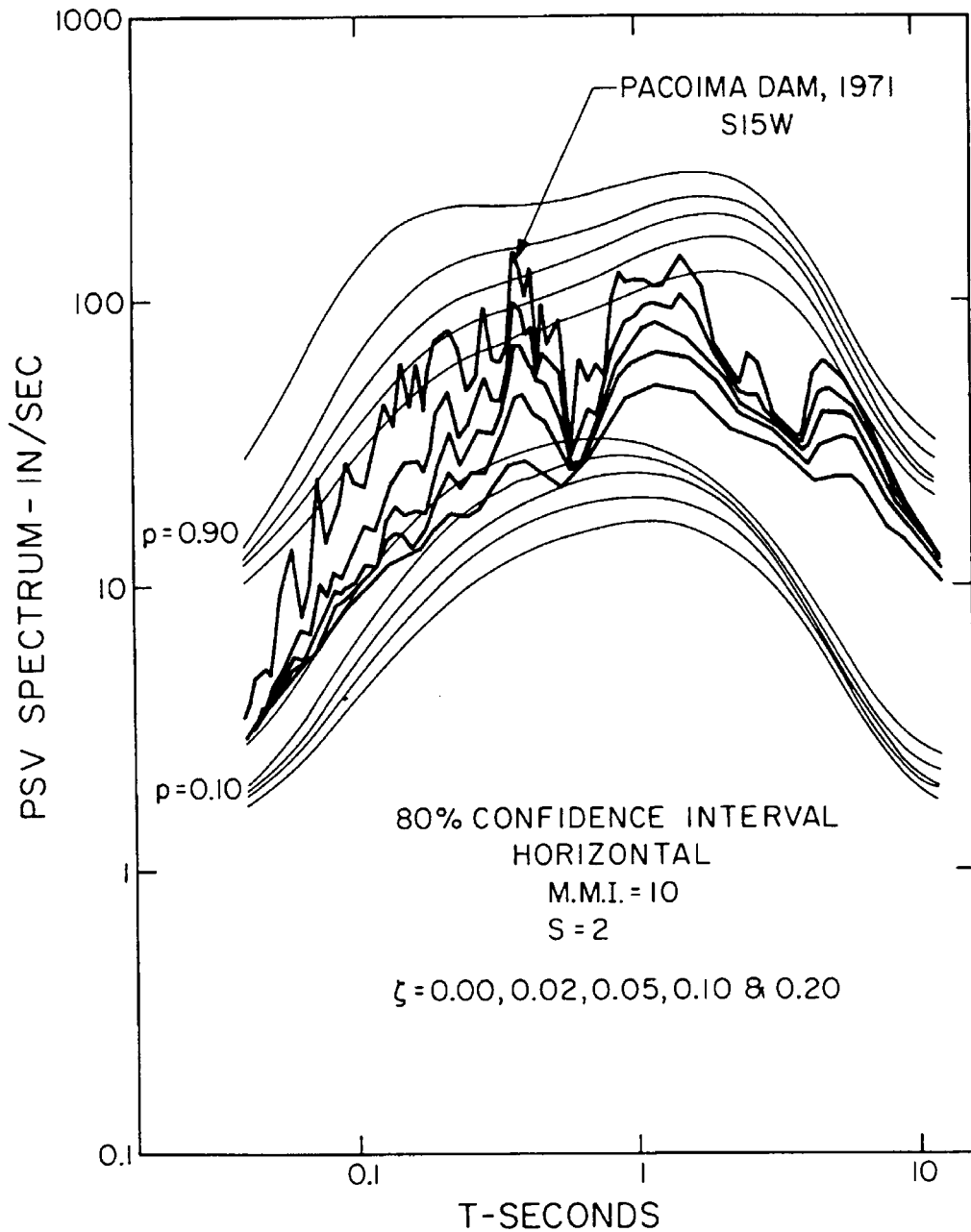
Fig. 10 Comparison of recorded (heavy lines) and computed (light lines) PSV spectra for 80% confidence interval

The new frequency-dependent attenuation function (Trifunac and Lee, 1985a) is

$$Att(\Delta, M, T) = Att_0(T)\log_{10}\Delta \tag{6a}$$

where $Att_0(T)$ is a parabola for $T < 1.8$ s and a constant for $T > 1.8$ s, as follows:

$$Att_0(T) = \begin{cases} -0.732025 & T > 1.8 \ s \\ a + b\log_{10}T + c(\log_{10}T)^2 & T < 1.8 \ s \end{cases} \tag{6b}$$

with $a = -0.767093$, $b = 0.271556$ and $c = -0.52564$ (see Figure 9.8 in Trifunac and Lee, 1985a). Δ is given by

$$\Delta = S\left(\ln \frac{R^2 + H^2 + S^2}{R^2 + H^2 + S_0^2} \right)^{-1/2} \tag{6c}$$

where

$$S = 0.2 + 8.51(M - 3) \tag{6d}$$

M is magnitude, and S_0 is defined as the correlation radius of the source function. S_0 can be approximated by $S_0 = C_s T/2$, where C_s is the shear wave velocity. The equations above result from Model III, selected by Trifunac and Lee (1985a) as the most suitable description of the frequency-dependent attenuation function.

The scaling functions $b_1(T)$ through $b_6(T)$ are determined through regression analysis. The data is first screened to minimize a possible bias in the model, which could result from uneven distribution of data among the different magnitude ranges and site conditions, or from excessive contribution to the database from several abundantly recorded earthquakes. All procedures in data preparation and selection, and the form of the regression analysis employed here are the same as in Trifunac and Lee (1985a), and thus, their description will not be repeated.

During the regression analysis, it was found that the linear term in Δ in Equation (5), namely $b_4(T)\Delta/100$, results in the coefficient $b_4(T)$ being insignificant for most of the periods. Subsequently, this term was deleted, and the scaling equation (Equation (5)) became

$$\log_{10}\left[PSV(T) \right] = M + Att(\Delta, M, T) + b_1(T)M + b_2(T)h + b_3(T)v + b_5(T) + b_6(T)M^2 \tag{7}$$

The resulting "coefficients" $b_i(T)$ at each period T, resulting from linear regression, will be denoted by $\hat{b}_1(T)$ through $\hat{b}_6(T)$, respectively. The regression analysis was carried out separately for 5 sets of pseudo relative velocity amplitudes corresponding to 5 different values of critical damping, $\zeta = 0.0, 0.02, 0.05, 0.10$ and 0.20.

If $\hat{b}_1(T)$ through $\hat{b}_6(T)$ represent the best estimates of the functions $b_1(T)$ through $b_6(T)$, then $\log_{10} P\hat{S}V(T)$ represents the best estimate of $\log_{10} PSV(T)$ at the same period T, where

$$\log_{10}\left[P\hat{S}V(T) \right] = M + Att(\Delta, M, T) + \hat{b}_1(T)M + \hat{b}_2(T)h + \hat{b}_3(T)v + \hat{b}_5(T) + \hat{b}_6(T)M^2 \tag{8}$$

For given values of T, h, v, and Δ, $\log_{10}\left[PSV(T) \right]$ represents a parabola, when plotted versus M. Following all preceding analyses, it was again assumed that Equation (8) applies only in the range $M_{min} \le M \le M_{max}$, where

$$M_{min} = -\hat{b}_1(T)/\left(2\hat{b}_6(T) \right) \text{ and } M_{max} = -\left(1 + \hat{b}_1(T) \right)/\left(2\hat{b}_6(T) \right) \tag{9}$$

For $M \le M_{min}$, M is used only in the first term of Equation (8), and M_{min} is used with $\hat{b}_1(T)$ and $\hat{b}_6(T)$. For $M \ge M_{max}$, M_{max} is used in all the terms of M. In other words, Equation (8) is modified to

$$\log_{10} P\hat{S}V(T) = Att(\Delta, M, T) + $$
$$\begin{cases} M + \hat{b}_1(T)M_{min} + \hat{b}_2(T)h + \hat{b}_3(T)v + \hat{b}_5(T) + \hat{b}_6(T)M_{min}^2, & M \le M_{min} \\ M + \hat{b}_1(T)M + \hat{b}_2(T)h + \hat{b}_3(T)v + \hat{b}_5(T) + \hat{b}_6(T)M^2, & M_{min} \le M \le M_{max} \\ M_{max} + \hat{b}_1(T)M_{max} + \hat{b}_2(T)h + \hat{b}_3(T)v + \hat{b}_5(T) + \hat{b}_6(T)M_{max}^2, & M_{max} \le M \end{cases} \tag{10}$$

This will result in linear growth of $\log_{10} PSV(T)$ with M for $M \le M_{min}$, in parabolic growth for $M_{min} \le M \le M_{max}$, and in a constant value of $PSV(T)$ corresponding to M_{max}, for $M \ge M_{max}$.

Table 1(a): PSV Regression Coefficients; Mag-Depth Model

$$\log_{10} \text{PSV}(T) = M + \text{At t}(\Delta, M, T) + b_1(T)M + b_2(T)h + b_3(T)v + b_5(T) + b_6(T)M^2$$

	Period, T (s)
	0.040	0.065	0.110	0.190	0.340	0.500	0.900	1.600	2.800	4.400	7.500	14.00
$\zeta = 0.00$												
$b_1(T)$	-0.021	-0.018	0.070	0.237	0.408	0.505	0.651	0.786	0.839	0.747	0.407	-0.276
$b_2(T)$	0.039	0.030	0.027	0.035	0.052	0.063	0.076	0.088	0.097	0.095	0.079	0.046
$b_3(T)$	-0.076	-0.024	-0.002	-0.029	-0.090	-0.130	-0.153	-0.125	-0.100	-0.108	-0.121	-0.091
$b_5(T)$	-1.580	-1.465	-1.747	-2.470	-3.345	-3.877	-4.627	-5.205	-5.341	-4.924	-3.693	-1.442
$b_6(T)$	-0.041	0.045	-0.054	-0.066	-0.076	-0.082	-0.091	-0.101	-0.108	-0.106	-0.086	-0.038
M_{min}	0.000	0.000	0.648	1.795	2.684	3.079	3.577	3.891	3.884	3.524	2.366	0.000
M_{max}	11.939	10.911	9.907	9.371	9.263	9.177	9.071	8.842	8.514	8.241	8.180	9.526
$\zeta = 0.02$												
$b_1(T)$	-0.036	-0.009	0.121	0.331	0.497	0.555	0.638	0.768	0.852	0.780	0.407	-0.097
$b_2(T)$	0.039	0.032	0.028	0.034	0.047	0.055	0.066	0.079	0.093	0.095	0.083	0.051
$b_3(T)$	-0.104	-0.061	-0.037	-0.049	-0.097	-0.134	-0.160	-0.135	-0.110	-0.115	-0.127	-0.102
$b_5(T)$	-1.630	-1.571	-1.954	-2.786	-3.645	-4.067	-4.632	-5.186	-5.400	-5.046	-3.951	-2.066
$b_6(T)$	-0.040	0.049	-0.064	-0.079	-0.089	-0.090	-0.094	-0.102	-0.112	-0.110	-0.092	0.052
M_{min}	0.000	0.000	0.945	2.095	2.792	3.083	3.394	3.765	3.804	3.545	2.603	0.000
M_{max}	12.050	10.112	8.758	8.424	8.410	8.639	8.713	8.667	8.268	8.091	8.038	8.683
$\zeta = 0.05$												
$b_1(T)$	-0.040	-0.003	0.131	0.344	0.517	0.571	0.628	0.728	0.807	0.764	0.538	0.092
$b_2(T)$	0.042	0.037	0.032	0.034	0.044	0.052	0.065	0.078	0.090	0.091	0.080	0.053
$b_3(T)$	-0.101	-0.072	-1.054	-0.062	-0.103	-0.140	-0.168	-0.143	-0.114	-0.117	-0.131	-1.113
$b_5(T)$	-1.697	-1.672	-2.060	-2.889	-3.750	-4.154	-4.638	-5.099	-5.296	-5.026	-4.167	-2.723
$b_6(T)$	-0.038	0.049	-0.065	-0.082	-0.092	-0.094	-0.094	-0.101	-0.109	-0.110	-0.097	0.068
M_{min}	0.000	0.000	1.008	2.098	2.810	3.037	3.340	3.604	3.702	3.473	2.773	0.676
M_{max}	12.632	10.173	8.700	8.195	8.245	8.356	8.660	8.554	8.289	8.018	7.928	8.029
$\zeta = 0.10$												
$b_1(T)$	0.007	-0.016	0.128	0.334	0.508	0.558	0.603	0.700	0.787	0.762	0.581	0.241
$b_2(T)$	0.043	0.038	0.033	0.035	0.044	0.052	0.064	0.076	0.087	0.089	0.079	0.049
$b_3(T)$	-0.105	-0.080	-0.062	-0.067	-0.107	-0.144	-0.175	-0.153	-0.123	-0.124	-0.138	-0.132
$b_5(T)$	-1.867	-1.809	-2.160	-2.960	-3.795	-4.171	-4.605	-5.047	-5.265	-5.044	-4.336	-3.229
$b_6(T)$	-0.041	0.049	-0.064	-0.081	-0.092	-0.094	-0.094	-0.100	-0.109	-0.111	-0.102	-0.079
M_{min}	0.085	0.163	1.000	2.062	2.761	2.968	3.207	3.500	3.610	3.432	2.848	1.525
M_{max}	12.280	10.367	8.813	8.235	8.196	8.287	8.527	8.500	8.197	7.937	7.750	7.854
$\zeta = 0.20$												
$b_1(T)$	0.092	0.063	0.136	0.315	0.473	0.520	0.555	0.637	0.732	0.739	0.616	0.338
$b_2(T)$	0.046	0.042	0.038	0.039	0.046	0.053	0.063	0.074	0.087	0.091	0.081	0.049
$b_3(T)$	-0.094	-0.085	-0.078	-0.082	-0.110	-0.139	-0.170	-0.157	-0.128	-0.120	-0.131	-0.150
$b_5(T)$	-2.151	-2.044	-2.322	-3.035	-3.803	-4.150	-4.528	-4.906	-5.144	-5.036	-4.511	-3.575
$b_6(T)$	-0.048	0.052	-0.063	-0.079	-0.089	-0.091	-0.091	-0.096	-0.106	-0.111	-0.105	-0.088
M_{min}	0.958	0.606	1.079	1.994	2.657	2.857	3.049	3.318	3.453	3.329	2.933	1.920
M_{max}	11.375	10.221	9.016	8.323	8.275	8.352	8.544	8.526	8.170	7.833	7.695	7.602

With $\text{PSV}(T)$ being the pseudo relative velocity response spectrum amplitudes computed from recorded accelerograms, the residuals $\varepsilon(T)$ were calculated from

$$\varepsilon(T) = \log_{10} \text{PSV}(T) - \log_{10} \hat{\text{PSV}}(T) \tag{11}$$

These residuals describe the distribution of the observed $\text{PSV}(T)$ about the estimated $\hat{\text{PSV}}(T)$. It is assumed that the residuals, $\varepsilon(T)$, can be described by the following probability distribution function of the form

$$p(\varepsilon, T) = \left[1 - \exp\left(- \exp\left(\alpha(T)\varepsilon(T) + \beta(T)\right)\right) \right]^{N(T)} \tag{12}$$

where, $p(\varepsilon, T)$ represents the probability that $\log_{10}[\text{PSV}(T)] - \log_{10}[\hat{\text{PSV}}(T)] \leq \varepsilon(T)$. $\alpha(T)$, $\beta(T)$ and $N(T)$ are parameters of the distribution function. The integer power $N(T)$ is estimated from the empirical equation

$$N(T) = \min(10, [25/T])$$ (13)

where, $[25/T]$ is the integral part of $25/T$. The parameters $\alpha(T)$ and $\beta(T)$ can then be estimated from the following equation, which is derived from Equation (12):

$$\ln\left(-\ln\left(1 - p^{1/N(T)}\right)\right) = \alpha(T)\varepsilon(T) + \beta(T)$$ (14)

For a given residual value $\varepsilon(T)$ at a particular period T, the actual probability $p*(\varepsilon, T)$ that $\varepsilon(T)$ will not be exceeded, can be evaluated by finding the fraction or residuals $\varepsilon(T)$ (computed from the database at that particular period) which are smaller than the given value. Using Equation (12), the estimated probability $\hat{p}(\varepsilon, T)$ that $\varepsilon(T)$ will not be exceeded, can also be evaluated and compared with the above fractions. The Kolmogorov-Smirnov, $KS(T)$, test and the χ^2 statistic, $\chi^2(T)$, can be computed to test for the goodness-of-fit of the distribution function in Equation (12).

Table 1(b): PSV Residuals Probability Coefficients (Equation (12)) and Goodness-of-Fit Statistics; Mag-Depth Model

$$\log_{10} \mathrm{PSV}(T) = M + \mathrm{Att}(\Delta, M, T) + \hat{b}_1(T)M + \hat{b}_2(T)h + \hat{b}_3(T)v + \hat{b}_5(T) + \hat{b}_6(T)M^2 + \varepsilon(T)$$

	Period, T (s)											
	0.040	0.065	0.110	0.190	0.340	0.500	0.900	1.600	2.800	4.400	7.500	14.00
$\zeta = 0.00$												
$\alpha(T)$	1.258	1.259	1.224	1.212	1.258	1.297	1.296	1.235	1.327	1.673	2.373	3.216
$\beta(T)$	1.027	1.006	1.006	1.007	1.000	0.998	1.013	1.018	0.935	0.767	0.492	0.197
$N(T)$	10	10	10	10	10	10	10	10	9	6	3	2
$\chi^2(T)$	7.082	7.305	7.932	8.732	9.581	9.905	10.040	9.632	9.340	9.645	10.662	12.244
$KS(T)$	0.029	0.028	0.028	0.031	0.034	0.036	0.036	0.037	0.041	0.046	0.052	0.058
$\zeta = 0.02$												
$\alpha(T)$	1.316	1.334	1.290	1.252	1.279	1.316	1.317	1.253	1.340	1.696	2.441	3.377
$\beta(T)$	1.027	1.008	1.008	1.010	1.002	0.999	1.014	1.019	0.935	0.767	0.492	0.197
$N(T)$	10	10	10	10	10	10	10	10	9	6	3	2
$\chi^2(T)$	6.469	7.455	8.893	10.657	11.502	11.011	9.430	8.484	8.648	9.331	11.005	14.718
$KS(T)$	0.028	0.028	0.030	0.034	0.038	0.039	0.038	0.037	0.040	0.044	0.050	0.057
$\zeta = 0.05$												
$\alpha(T)$	1.320	1.360	1.324	1.273	1.282	1.315	1.321	1.263	1.358	1.731	2.520	3.526
$\beta(T)$	1.028	1.008	1.008	1.010	1.003	1.000	1.014	1.018	0.934	0.767	0.494	0.200
$N(T)$	10	10	10	10	10	10	10	10	9	6	3	2
$\chi^2(T)$	5.817	6.723	8.450	10.117	10.566	10.250	10.033	10.752	11.395	11.192	10.455	10.164
$KS(T)$	0.026	0.028	0.031	0.034	0.037	0.038	0.039	0.041	0.045	0.048	0.050	0.051
$\zeta = 0.10$												
$\alpha(T)$	1.326	1.382	1.356	1.302	1.296	1.318	1.312	1.258	1.376	1.772	2.573	3.558
$\beta(T)$	1.028	1.009	1.009	1.011.	1.003	1.001	1.015	1.018	0.932	0.766	0.496	0.210
$N(T)$	10	10	10	10	10	10	10	10	9	6	3	2
$\chi^2(T)$	5.224	6.504	8.149	9.531	9.910	9.715	9.476	9.314	8.660	8.267	9.518	14.031
$KS(T)$	0.025	0.027	0.030	0.034	0.038	0.039	0.037	0.036	0.039	0.045	0.050	0.052
$\zeta = 0.20$												
$\alpha(T)$	1.307	1.377	1.368	1.325	1.312	1.321	1.307	1.277	1.432	1.848	2.646	3.618
$\beta(T)$	1.028	1.010	1.010	1.011	1.003	1.001	1.016	1.019	0.933	0.767	0.500	0.218
$N(T)$	10	10	10	10	10	10	10	10	9	6	3	2
$\chi^2(T)$	5.127	6.602	8.300	9.740	10.685	10.873	10.512	9.950	9.756	9.605	8.770	6.936
$KS(T)$	0.026	0.029	0.034	0.037	0.039	0.039	0.039	0.038	0.040	0.043	0.047	0.049

1.2 Results of the Regression Analysis

Table 1 gives, for 12 points between $T = 0.04$ and $T = 14$ s, the amplitudes of the smoothed regression coefficients $\hat{b}_1(T)$, $\hat{b}_2(T)$, $\hat{b}_3(T)$, $\hat{b}_5(T)$, $\hat{b}_6(T)$ (note that $b_4(T)$ has been deleted), $\hat{M}_{\min}(T)$, $\hat{M}_{\max}(T)$, the smoothed amplitudes of $N(T)$, $\hat{\alpha}(T)$, $\hat{\beta}(T)$ in Equation (12), and the χ^2 and Kolmogorov-Smirnov statistics. The 12 periods used appear to be sufficient for most practical

computations, since the smoothness of PSV is such that almost any interpolation scheme will yield adequate estimates of their amplitudes at any period in the range $0.04 - 15$ s.

Table 2(a): PSV Regression Coefficients; MMI-Depth Model

$$\log_{10} \text{PSV}(T) = b_1(T)I_{MM} + b_2(T)h + b_3(T)v + b_4(T)$$

	Period, T (s)											
	0.040	0.065	0.110	0.190	0.340	0.500	0.900	1.600	2.800	4.400	7.500	14.00
$\zeta = 0.00$												
$b_1(T)$	0.223	0.231	0.257	0.297	0.332	0.341	0.335	0.315	0.283	0.248	0.201	-0.145
$b_2(T)$	-0.027	-0.023	0.009	0.017	0.050	0.069	0.088	0.096	0.097	0.089	0.070	0.036
$b_3(T)$	-0.061	-0.029	-0.015	-0.045	-0.109	-0.139	-0.135	-0.099	-0.082	-0.039	-0.107	-0.115
$b_4(T)$	-1.715	-1.464	-1.278	-1.284	-1.435	-1.524	-1.551	-1.434	-1.207	-0.983	-0.757	-0.612
$\zeta = 0.02$												
$b_1(T)$	0.208	0.213	0.241	0.289	0.333	0.348	0.347	0.328	0.294	0.259	0.211	0.158
$b_2(T)$	-0.023	-0.026	-0.020	0.001	0.033	0.054	0.076	0.086	0.090	0.086	0.070	0.036
$b_3(T)$	-0.093	-0.066	-0.048	-0.067	-0.122	-0.152	-0.153	-0.117	-0.093	-0.099	-0.120	-0.132
$b_4(T)$	-1.766	-1.540	-1.393	-1.441	-1.625	-1.726	-1.756	-1.630	-1.383	-1.142	-0.900	-0.747
$\zeta = 0.05$												
$b_1(T)$	0.213	0.215	0.238	0.283	0.328	0.344	0.347	0.333	0.305	0.271	0.223	0.168
$b_2(T)$	-0.024	-0.025	-0.019	0.000	0.031	0.050	0.071	0.083	0.088	0.086	0.072	0.041
$b_3(T)$	-0.101	-0.080	-0.064	-0.077	-0.126	-0.155	-0.163	-0.134	-0.112	-0.116	-0.135	-0.148
$b_4(T)$	-1.824	-1.607	-1.466	-1.513	-1.694	-1.798	-1.845	-1.746	-1.521	-1.286	-1.040	-0.876
$\zeta = 0.10$												
$b_1(T)$	0.219	0.219	0.239	0.281	0.324	0.340	0.345	0.333	0.308	0.278	0.235	0.185
$b_2(T)$	-0.025	-0.023	-0.017	-0.001	-0.027	0.046	0.069	0.082	0.086	0.083	0.070	0.043
$b_3(T)$	-0.102	-0.087	-0.075	-0.086	-0.129	-0.157	-0.165	-0.137	-0.114	-0.117	-0.139	-0.158
$b_4(T)$	-1.882	-1.682	-1.551	-1.597	-1-769	-1.869	-1.921	-1.838	-1.634	-1.417	-1.190	-1.039
$\zeta = 0.20$												
$b_1(T)$	0.226	0.228	0.245	0.280	0.319	0.335	0.343	0.331	0.308	0.282	0.245	0.199
$b_2(T)$	-0.022	-0.024	-0.018	0.000	0.027	0.043	0.062	0.073	0.079	0.079	0.068	0.043
$b_3(T)$	-0.102	-0.093	-0.086	-0.096	-0.132	-0.157	-0.168	-0.143	-0.117	-0.117	-0.140	-0.161
$b_4(T)$	-1.960	-1.791	-1.675	-1.708	-1.862	-1.956	-2.004	-1.920	-1.735	-1.550	-1.355	-1.205

2. Scaling of $\text{PSV}(T)$ in Terms of M, R, H, S, s and v

Sub-section 1 above characterized the local geology by the approximate overall depth of sedimentary deposits beneath the recording station, h, in km. As it has been noted previously, while the depth of sediments at each recording station represents a preferable site characterization, in many instances, little may be known about such depth at some sites, and so, the scaling of PSV amplitudes at any such site using depth, h, would become impossible. The site characterization in terms of $s = 0, 1$ and 2, which can be determined from knowledge of surface geology only, thus remains a useful approach to the scaling of PSV amplitudes. For a description of the distribution of data in the database (of early 1980's) among the different site conditions, and for the associated regression analyses, the reader is referred to Trifunac and Lee (1985b, 1985c).

3. Scaling of $\text{PSV}(T)$ in Terms of MMI, h and v

3.1 The Scaling Relation

Sub-sections 1 and 2 above presented the description of the empirical models for scaling pseudo relative velocity spectra from strong-motion earthquake acceleration in terms of earthquake magnitude, source-to-station representative distance, and a parametric characterization of local geology at the recording station. Following the approach of Trifunac and Lee (1985b) for the scaling of Fourier amplitude spectra, Sub-sections 3 and 4 summarize the extension of the method outlined above to the scaling of pseudo relative velocity spectra in terms of Modified Mercalli Intensity (MMI) at the site.

The scaling equation becomes (Equation (4) of Trifunac and Lee (1979))

$$\log_{10}[\text{PSV}(T)] = b(T)I_{MM} + c(T) + d(T)h + e(T)v \tag{15}$$

with I_{MM} denoting the reported discrete levels of the MMI scale at the recording station, and with all other parameters defined as above.

Table 2(b): PSV Residuals Probability Coefficients (Equation (12)) and Goodness-of-Fit Statistics; MMI-Depth Model

$$\log_{10} \mathrm{PSV}(T) = \hat{b}_1(T)I_{MM} + \hat{b}_2(T)h + \hat{b}_3(T)v + \hat{b}_4(T) + \varepsilon(T)$$

	Period, T (s)											
	0.040	0.065	0.110	0.190	0.340	0.500	0.900	1.600	2.800	4.400	7.500	14.00
$\zeta = 0.00$												
$\alpha(T)$	1.061	1.096	1.126	1.167	1.194	1.181	1.055	1.055	1.219	1.605	2.288	3.066
$\beta(T)$	1.006	0.987	0.988	0.991	0.984	0.982	0.998	1.004	0.919	0.752	0.484	0.204
$N(T)$	10	10	10	10	10	10	10	10	9	6	3	2
$\chi^2(T)$	6.623	6.878	6.162	5.342	5.695	6.804	9.229	11.205	11.654	11.103	10.743	12.511
$KS(T)$	0.029	0.030	0.028	0.026	0.027	0.030	0.037	0.044	0.046	0.046	0.048	0.057
$\zeta = 0.0$												
$\alpha(T)$	1.139	1.159	1.165	1.193	1.236	1.241	1.183	1.121	1.267	1.653	2.359	3.176
$\beta(T)$	1.006	0.988	0.988	0.990	0.983	0.981	0.998	1.004	0.918	0.751	0.482	0.201
$N(T)$	10	10	10	10	10	10	10	10	9	6	3	2
$\chi^2(T)$	6.993	6.994	6.332	5.340	4.813	5.254	7.703	11.571	14.225	13.897	10.959	7.452
$KS(T)$	0.026	0.028	0.028	0.026	0.026	0.028	0.036	0.046	0.052	0.053	0.051	0.053
$\zeta = 0.05$												
$\alpha(T)$	1.176	1.194	1.186	1.202	1.249	1.264	1.217	1.152	1.295	1.688	2.413	3.249
$\beta(T)$	1.005	0.988	0.989	0.990	0.982	0.981	0.999	1.005	0.918	0.750	0.480	0.199
$N(T)$	10	10	10	10	10	10	10	10	9	6	3	2
$\chi^2(T)$	6.204	6.645	6.978	6.765	6.353	6.669	8.840	12.064	13.805	13.170	10.981	9.395
$KS(T)$	0.026	0.028	0.029	0.028	0.028	0.031	0.038	0.047	0.052	0.051	0.048	0.048
$\zeta = 0.10$												
$\alpha(T)$	1.211	1.231	1.215	1.216	1.256	1.276	1.244	1.195	1.341	1.725	2.425	3.231
$\beta(T)$	1.004	0.988	0.989	0.991	0.983	0.982	1.000	1.006	0.919	0.749	0.477	0.192
$N(T)$	10	10	10	10	10	10	10	10	9	6	3	2
$\chi^2(T)$	5.610	6.922	8.055	7.692	6.527	6.895	10.477	14.973	15.972	13.727	10.199	8.859
$KS(T)$	0.033	0.032	0.031	0.030	0.029	0.031	0.038	0.046	0.050	0.049	0.047	0.048
$\zeta = 0.20$												
$\alpha(T)$	1.251	1.277	1.259	1.250	1.277	1.290	1.254	1.220	1.394	1.787	2.458	3.190
$\beta(T)$	1.004	0.988	0.990	0.991	0.983	0.982	1.000	1.006	0.918	0.748	0.473	0.185
$N(T)$	10	10	10	10	10	10	10	10	9	6	3	2
$\chi^2(T)$	6.768	7.540	7.114	5.810	5.839	7.512	11.826	15.594	16.616	15.203	11.806	7.674
$KS(T)$	0.037	0.037	0.033	0.027	0.025	0.028	0.040	0.053	0.059	0.056	0.050	0.049

The analysis was next carried out on the database with 438 free-field records from 104 earthquakes. The estimated MMI levels at some of the 438 free-field sites were used in addition to the reported MMI levels, which for the most part were available only for the original 186 free-field sites. The estimated MMI levels have been calculated by using the scaling equation

$$I_{MM} = 1.5M - A - B\ln\Delta - C\Delta/100 - Ds \qquad (16)$$

with the procedure, as described in Lee and Trifunac (1985).

The scaling of pseudo relative velocity spectra now takes the form

$$\log_{10}\left[\mathrm{PSV}(T)\right] = b_1(T)\hat{I}_{MM} + b_2(T)h + b_3(T)v + b_4(T) \qquad (17)$$

where $\hat{I}_{MM}$ is the estimated MMI level at the site from Equation (16), or the reported MMI level there, if available.

The scaling functions $b_1(T)$ through $b_4(T)$ have been determined through the regression analysis of the database. The fitted coefficients at each period T resulting from linear regression are denoted by $\hat{b}_1(T)$, $\hat{b}_2(T)$, $\hat{b}_3(T)$ and $\hat{b}_4(T)$.

3.2 Results of the Regression Analysis

Substitution of the coefficients $\hat{b}_1(T)$, $\hat{b}_2(T)$ into Equation (17) gives $\hat{\text{PSV}}(T)$:

$$\log_{10} \hat{\text{PSV}}(T) = \hat{b}_1(T)I_{MM} + \hat{b}_2(T)h + \hat{b}_3(T)v + \hat{b}_4(T) \tag{18}$$

where, $\log_{10} \hat{\text{PSV}}(T)$ represents the estimate of the logarithm of the pseudo relative velocity spectrum at period T for this model. We recall Equation (8):

$$\log_{10}\left[\text{PSV}(T)\right] = M + \text{Att}(\Delta, M, T) + \hat{b}_1(T)M + \hat{b}_2(T)h + \hat{b}_3(T)v + \hat{b}_5(T) + \hat{b}_6(T)M^2 \tag{19}$$

which corresponds to the scaling of $\text{PSV}(T)$ in terms of magnitude M, and "representative" source-to-station distance Δ. Trifunac and Lee (1985a, 1985b, 1985c, 1987) have described the resemblance in shape, of the function $\hat{b}_1(T)$ for intensity I_{MM} in (18), and M in Equation (19). The same holds true for the scaling function $\hat{b}_2(T)$ for h, and $\hat{b}_3(T)$ for v in both equations. This resemblance is obvious, even though, unlike in Equation (19), the explicit dependence of $\text{PSV}(T)$ on "representative" source-to-station distance, Δ, is omitted from Equation (18). As pointed out previously (Trifunac and Lee, 1979), Equation (18) is intended to be in such simple form. Including the explicit dependence of $\text{PSV}(T)$ on epicentral distance, R, or on "representative" source-to-station distance, Δ, as in $\text{Att}(\Delta, M, T)$, would decrease the uncertainties associated with the estimation of $\text{PSV}(T)$ in Equation (19), but then, this equation would only be applicable to those regions which have similar intensity attenuation with distance, as in California, where over 90% of the records in the database have been recorded.

With $\text{PSV}(T)$ being the pseudo relative velocity with the damping value $\zeta = 0$, and computed from recorded accelerograms, the residuals, $\varepsilon(T)$, were calculated from Equation (11). It is assumed here again that the residuals, $\varepsilon(T)$ can be described by the distribution function of the form given by Equation (12). The probability $p(\varepsilon, T)$ at period T that $\log_{10} \text{PSV}(T) - \log_{10} \hat{\text{PSV}}(T) \leq \varepsilon(T)$, is then given by Equation (12), with $\alpha(T)$ and $\beta(T)$ being the parameters to be determined. The integer power $N(T)$ in Equation (12) was estimated from the empirical equation, Equation (13).

For a given residue $\varepsilon(T)$ at a particular period T, the actual probability $p*(\varepsilon, T)$ that $\varepsilon(T)$ will not be exceeded, the corresponding estimated probability $\hat{p}(\varepsilon, T)$, the Kolmogorov-Smirnov statistic, $KS(T)$, and the χ^2 statistic, $\chi^2(T)$, are all computed as in Sub-section 1 above, where a complete description of the steps and formulae involved are also described.

Tables 2(a) and 2(b) give, for 12 periods between $T = 0.04$ s and $T = 14$ s, the amplitudes of the smoothed regression coefficients $\hat{b}_1(T)$ through $\hat{b}_4(T)$, the discrete values $N(T)$, the smoothed coefficients $\hat{\alpha}(T)$ and $\hat{\beta}(T)$ in Equation (12), and the $\chi^2(T)$ and $KS(T)$ statistics.

4. Scaling of $\text{PSV}(T)$ in Terms of MMI, s and v

Next, the description of the empirical model of scaling pseudo relative velocity spectra, computed from strong ground motion, in terms of Modified Mercalli Intensity (MMI) at a site and a description of local site geology can be considered. As in Sub-section 2 above, this analysis replaces the depth of sedimentary deposits h, used for the site characterization in Sub-section 3, by the corresponding site parameter s $(s = 0, 1 \text{ and } 2)$. The scaling relation and the results of regression analysis can be found in Trifuanc and Lee (1985c).

FREQUENCY-PATH-DEPENDENT ATTENUATION AND SIMULTANEOUS TREATMENT OF GEOLOGICAL AND SOIL SITE CONDITIONS

Starting in early 1990's, the frequency and magnitude-dependent attenuation equations of Trifunac and Lee (1985a) were further improved to include variations among selected "typical" wave paths. This enabled development of, so far the most advanced (third generation), empirical scaling equations of peak amplitudes (Lee et al., 1995) and spectra (Lee and Trifunac, 1995a, 1995b) of recorded strong ground motion. These developments were made possible by rapid increase in the number and quality of uniformly processed strong motion data.

1.   The New (Current) Strong Motion Database

By late-1993, strong motion database grew to over 1926 free-field records from 297 earthquakes and aftershocks. This corresponds to over 3800 horizontal components and 1900 vertical components.

For each record in this database, the following information has been collected: (1) coordinates (latitude and longitude) and address of the recording site, (2) epicentral, R, and hypocentral, D, distances, (3) component orientation, (4) local geological site classification, s, (5) depth of sediments, h, from the surface to geological basement rock beneath the site, (6) local soil type, s_L, representative of the top 100 m - 200 m beneath the surface (Trifunac, 1990a), where $s_L = 0$ for hard "rock" soil sites, $s_L = 1$ for stiff soil sites, $s_L = 2$ for deep soil sites, (7) average soil velocity, V_L, in the top 30 m beneath the surface (if this is not available, a soil velocity type, S_T, is used instead, such that for $V_L > .75$ km/s, $.75 \geq V_L > .36$ km/s, $.36 \geq V_L > .18$ km/s, and $V_L \leq .18$ km/s, it is assigned to indicator variables A, B, C or D, respectively), (8) r (or $100r$), the ratio (or percentage), $0 \leq r \leq 1$, of the wave path through geological basement rock to the total path, measured along the surface from the earthquake epicenter to the recording site, and (9) the generalized path type classification, describing different types of wave paths between the sources and stations. At present, we consider eight such categories. Figure 11 shows a plot of the schematic representations of the ``geometry'' of these path types.

With the above set of parameters available at each of the recording sites, scaling equations were developed by regression analyses of peak accelerations, velocities and displacements (Lee et al., 1995), and of the duration of strong ground motion (Novikova and Trifunac, 1995). A new frequency-dependent attenuation function and empirical scaling equations for Fourier amplitudes were also developed (Lee and Trifunac, 1995a). The new frequency-dependent attenuation function describes the attenuation of the Fourier amplitudes at each period from the source to the site. It takes the form (Trifunac and Lee, 1990)

$$\text{Att}(\Delta, M, T) = \begin{cases} A_0(T)\log(\Delta/L), & R \leq R_{\max} \\ A_0(T)\log(\Delta_{\max}/L) - (R - R_{\max})/200, & R > R_{\max} \end{cases} \tag{20}$$

with Δ, R, $\Delta_{\max}$, $R_{\max}$ defined as in the previous sections. The new parameter, $L = L(M)$, represents the length of the earthquake fault. It is approximately equal to $L = .01 \times 10^{0.5M}$ km (Trifunac, 1993a, 1993b). Δ/L is thus a dimensionless representative source-to-station distance.

At present, not all path types (Figure 11) have sufficient data to allow independent analyses. To ensure that the regression results are significant, several path types that are "similar" or "comparable", have been lumped into the following six groups: "0" includes all path types; "1" includes path type 1; "2" includes path types 2 and 6, "3" includes path types 3 and 7; "4" includes path types 4, 5 and 8; and "5" includes the path through rock only (path type 4). Regression analyses were then performed for each of the path groups (0 to 5) separately.

2.   New Scaling Equations of PSV Spectra

We illustrate here only the scaling equations for the regression of pseudo relative velocity (PSV) spectral amplitudes in terms of magnitude, site geology, local soil types, and percentage of rock along the wave path from source to station.
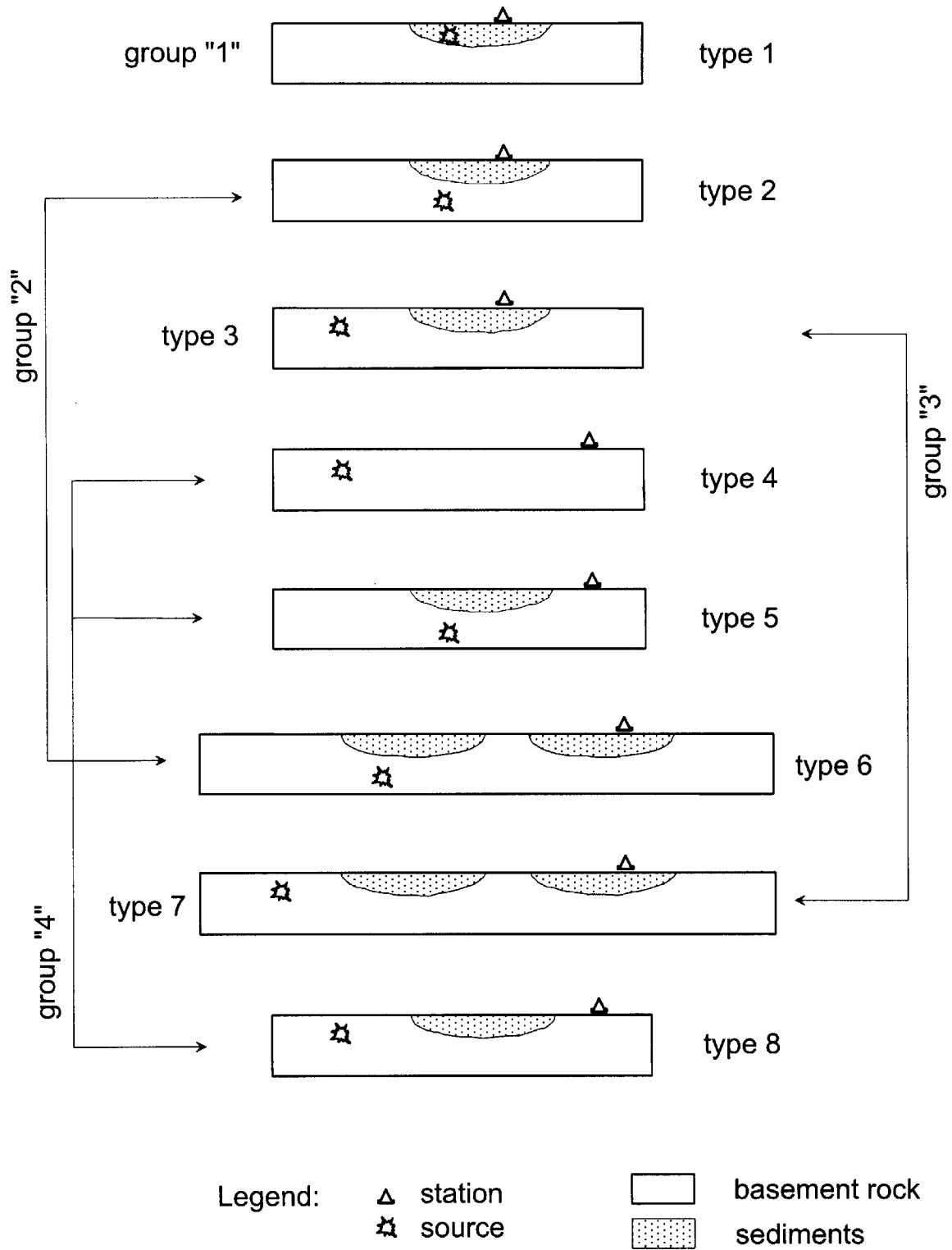
Fig. 11 Schematic representation of eight different path types for seismic waves propagating from source to the recording station (grouping of these eight path types into path groups, "1", "2", "3", ..., is also shown)

Regression equations of similar form were previously used for the analyses of peak acceleration, velocity and displacement (Lee et al., 1995). The same equations were used for the analyses of Fourier spectral amplitudes, $FS(T)$ (Lee and Trifunac, 1995a). The reader is referred to the above two reports for additional detailed description of the equations and of the steps involved in the execution of the regression analyses and development of the scaling models. The equations used for the four scaling models are:

Model (i): Mag-site + soil + % rock path multi-step model

$$\log PSV(T) = \begin{cases} M + A_0(T)\log(\Delta/L) + b_1(T)M + b_2(T)a + b_3(T)v + b_4(T) + b_5(T)M^2 \\ \quad + \sum_i b_6^{(i)}(T)S_L^{(i)} + \left(b_{70}(T)r + b_{71}(T)(1-r)\right)R \qquad\qquad R \le R_{max} \\ M + A_0(T)\log(\Delta_{max}/L) + b_1(T)M + b_2(T)a + b_3(T)v + b_4(T) + b_5(T)M^2 \\ \quad + \sum_i b_6^{(i)}(T)S_L^{(i)} + \left(b_{70}(T)r + b_{71}(T)(1-r)\right)R_{max} - (R - R_{max})/200 \quad R > R_{max} \end{cases}$$ (21)

Model (ii): Mag-depth + soil + % rock path multi-step model

$$\log PSV(T) = \begin{cases} M + A_0(T)\log(\Delta/L) + b_1(T)M + b_2(T)h + b_3(T)v + b_4(T) + b_5(T)M^2 \\ \quad + \sum_i b_6^{(i)}(T)S_L^{(i)} + \left(b_{70}(T)r + b_{71}(T)(1-r)\right)R \qquad\qquad R \le R_{max} \\ M + A_0(T)\log(\Delta_{max}/L) + b_1(T)M + b_2(T)h + b_3(T)v + b_4(T) + b_5(T)M^2 \\ \quad + \sum_i b_6^{(i)}(T)S_L^{(i)} + \left(b_{70}(T)r + b_{71}(T)(1-r)\right)R_{max} - (R - R_{max})/200 \quad R > R_{max} \end{cases}$$ (22)

Model (iii): Mag-site + no soil + % rock path multi-step model

$$\log PSV(T) = \begin{cases} M + A_0(T)\log(\Delta/L) + b_1(T)M + b_2(T)s + b_3(T)v + b_4(T) + b_5(T)M^2 \\ \quad + \left(b_{70}(T)r + b_{71}(T)(1-r)\right)R \qquad\qquad\qquad\qquad R \le R_{max} \\ M + A_0(T)\log(\Delta_{max}/L) + b_1(T)M + b_2(T)s + b_3(T)v + b_4(T) + b_5(T)M^2 \\ \quad + \left(b_{70}(T)r + b_{71}(T)(1-r)\right)R_{max} - (R - R_{max})/200 \qquad\quad R > R_{max} \end{cases}$$ (23)

Model (iv): Mag-depth + no soil + % rock path multi-step model

$$\log PSV(T) = \begin{cases} M + A_0(T)\log(\Delta/L) + b_1(T)M + b_2(T)h + b_3(T)v + b_4(T) + b_5(T)M^2 \\ \quad + \left(b_{70}(T)r + b_{71}(T)(1-r)\right)R \qquad\qquad\qquad\qquad R \le R_{max} \\ M + A_0(T)\log(\Delta_{max}/L) + b_1(T)M + b_2(T)h + b_3(T)v + b_4(T) + b_5(T)M^2 \\ \quad + \left(b_{70}(T)r + b_{71}(T)(1-r)\right)R_{max} - (R - R_{max})/200 \qquad\quad R > R_{max} \end{cases}$$ (24)

The frequency-dependent attenuation function, $A_0(T)\log(\Delta/L)$, used in each of the four models, is the function previously determined for the corresponding model in the regression of Fourier spectral amplitudes (Lee and Trifunac, 1995a). In Lee and Trifunac (1995a), notation $b_0(T)\log(\Delta/L)$ was used, to distinguish this from the similar terms in the second generation scaling models. The scaling functions $b_1(T)$ through $b_{71}(T)$ for each of the regression models were determined through regression analyses, using the new database of calculated $PSV(T)$ amplitudes of over 1900 free-field records, at 91 discrete periods T, ranging from 0.04 sec to 15 sec, and for damping ratio $\zeta = 0.05$.

Description of the detailed steps of regression analyses, and illustration of numerous tables and figures resulting from the above models, is far too voluminous to be included in this review. The reader may peruse the reports by Lee and Trifunac (1995a, 1995b) for further details.

EXTENSION OF EMPIRICAL SCALING EQUATIONS TO HIGH AND LOW FREQUENCIES

The spectrum amplitudes described by detailed empirical scaling equations (Lee, 1989, 1990, 1991) are needed in computation of uniform hazard in terms of relative response spectra, in the probabilistic site specific analyses leading to seismic micro- and macro-zonation (Trifunac, 1988, 1989d, 1990b). Response spectra are also used in probabilistic determination of envelopes of shear forces and of bending moments

in engineering design (Amini and Trifuanc, 1985; Gupta and Trifunac, 1988a, 1988b, 1990a, 1990b, 1991a, 1991b; Todorovska, 1994a, 1994b, 1994c), and in estimation of losses for buildings exposed to strong shaking (Jordanovski et al., 1993). In all this work, spectral amplitudes need to be specified in a broad frequency band, which is broader than the band where the empirical scaling equations are valid.

In this section, a method for extension of the empirical scaling equations for response spectrum amplitudes, to periods longer than several seconds and shorter than 0.04 s, is reviewed. The proposed extension functions for long periods will match with the empirical response spectral amplitudes at the frequencies where the empirical scaling equations are still valid, and will be consistent with other independent observations and estimates of strong motion.
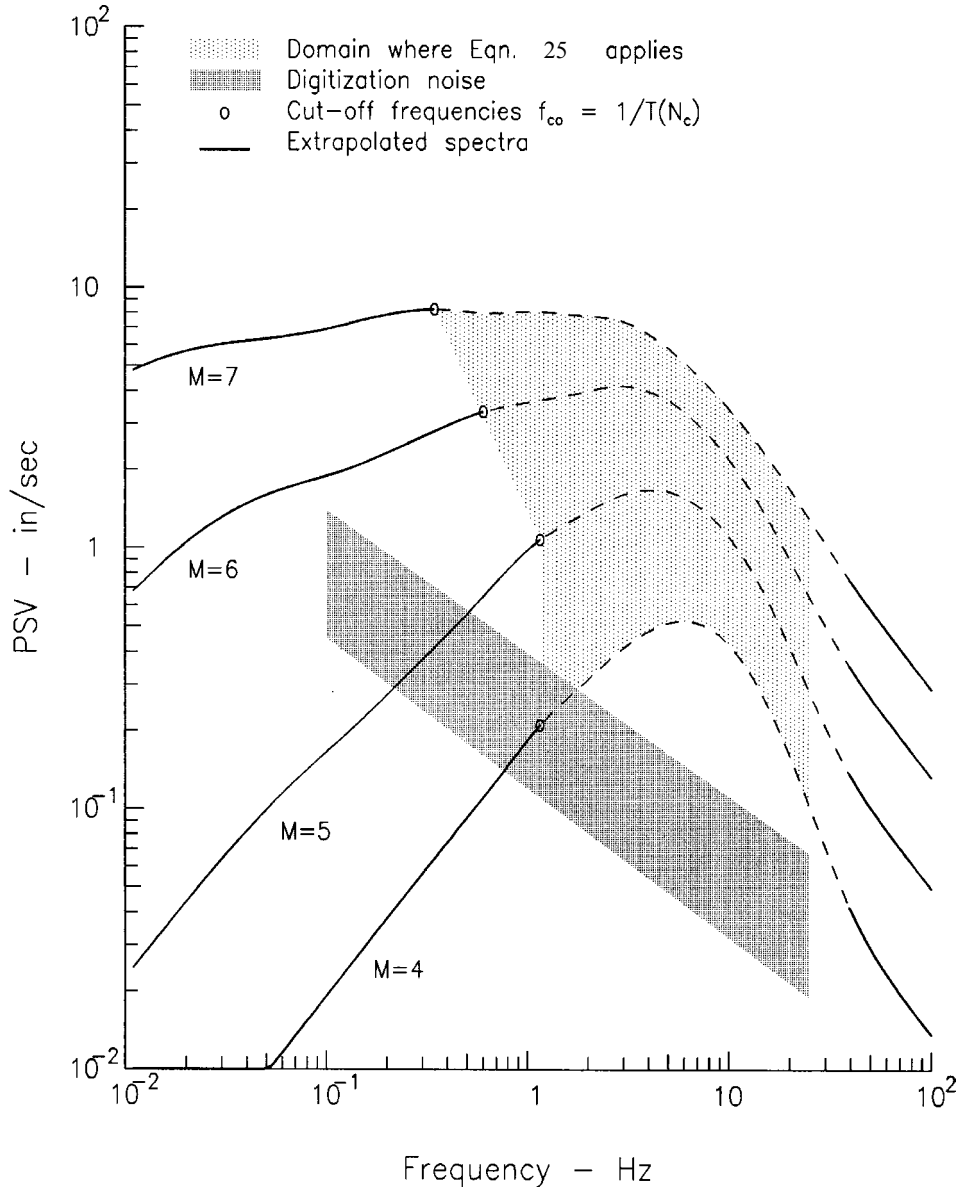
Fig. 12 PSV spectra versus frequency for damping ratio $\zeta = 0.05$ and probability of exceedance 0.5; the site is at epicentral distance $R = 10$ km and on rock $(h = 0)$, the source is at $H = 5$ km depth, and with magnitudes $M = 4, 5, 6$ and 7 (Equation (25) is valid inside the light shaded region for frequencies between corner frequency $f_{c0} = 1/T$ and 25 Hz; the extrapolation beyond this zone (heavy solid lines) is as proposed in this paper; the processing and digitization noise amplitudes are shown by the darker shaded zone increasing from ~10^{-1} to ~1 in/sec for frequencies decreasing from 10 to 0.1 Hz)

1. Empirical Scaling Equations

As we have shown in the previous sections, the empirical scaling equations for PSV spectral amplitudes employ scaling parameters, which depended on the earthquake source, propagation path and local site conditions. A typical equation is of the form

$$\log_{10}[\text{PSV}(T)] = f(M, \Delta, T, v, h, s_L) \tag{25}$$

where, M is the earthquake magnitude, Δ is the representative source-to-station distance, T is the period of motion, and $v = 0$ for horizontal and $v = 1$ for vertical motion. h represents the depth of sediments, and s_L is the soil classification parameter. Those describe the local site conditions (Trifunac, 1990a). When some of these parameters are not available, other related equations can be employed. For example, in place of M, the site intensity may be used.

Our ability to develop empirical scaling equations for $\text{PSV}(T)$ is limited by the quality and quantity of recorded strong motion data. As we have illustrated above, the preliminary scaling equations may be developed with several hundred recorded accelerograms. Frequency-dependent attenuation might be formulated with at least 500-600 records. More detailed scaling models will require at least one or two thousand records. The useful frequency range will depend on the characteristics of the recording transducers and on the digitization and processing techniques. Today, uniformly processed high quality strong motion data is available for periods between 0.04 and several seconds. This is illustrated in Figure 12, where the domain where Equation (25) applies, is indicated by the lightly shaded zone. This zone is bounded by spectra for $M = 4$ and $M = 7$, and lies between $T = 0.04$ s and T_c (cut-off period, increasing from 0.90 s for $M = 3$ and 4 to 7.5 s for $M = 7$ (Trifunac, 1993a)). The dark shaded zone, extending from $\sim 10^{-1}$ in/s near $T = 0.04$ s to ~ 1 in/s near $T = 10$ s, represents the amplitudes of the recording and processing noise (Trifunac and Todorovska, 2001a).

2. Long Period Extension

To extend $\text{PSV}(T)$ amplitudes to long periods, we consider two extreme situations. One is referred to as "far-field", in which it will be assumed that $(R^2 + H^2)^{1/2} >> L$, and the other is called "near-field" for $(R^2 + H^2)^{1/2} \leq L, W$. Here, L is the fault length, and W is the fault width. Finally, to compute $\text{PSV}(T)$ at any distance, we specify the weighting functions that measure the relative contribution of the "near-field" and "far-field" terms to the complete ground motion and to the corresponding $\text{PSV}(T)$ spectra.

The method will be identical to the one proposed for extrapolation of Fourier amplitude spectra to long periods (Trifunac, 1993a). In the first step, appropriate spectrum shape functions $\left(\dfrac{2\pi}{T} {}_F X_r(T,\zeta) \text{ and } \dfrac{2\pi}{T} {}_N X_r(T,\zeta) \right)$ are chosen. The amplitudes of these functions are next determined to agree with $\text{PSV}(T)$ amplitudes computed from regression equations, like Equation (25), at $T = T_c$. No attempt has been made to match the slopes of $\text{PSV}(T)$ for $T \leq T_c$ with $\dfrac{2\pi}{T} {}_F X_r(T,\zeta)$ or $\dfrac{2\pi}{T} {}_N X_r(T,\zeta)$ for $T \geq T_c$. Finally, the success of the extrapolation can be tested by comparing the results with other independent estimates of the appropriate scaling parameters or function amplitudes, as $T \to \infty$.

2.1 Far-Field Extension

Let $\left| {}_F X_r(T,\zeta) \right|_{\max}$ be the peak of relative response of a single-degree-of-freedom system with frequency $\omega = 2\pi/T$, and fraction of critical damping ζ. To develop a functional form of $\left| {}_F X_r(T,\zeta) \right|_{\max}$, which can be used to extend the PSV spectra in the "far-field" and for large T, Trifunac (1995a) considers a pulse,
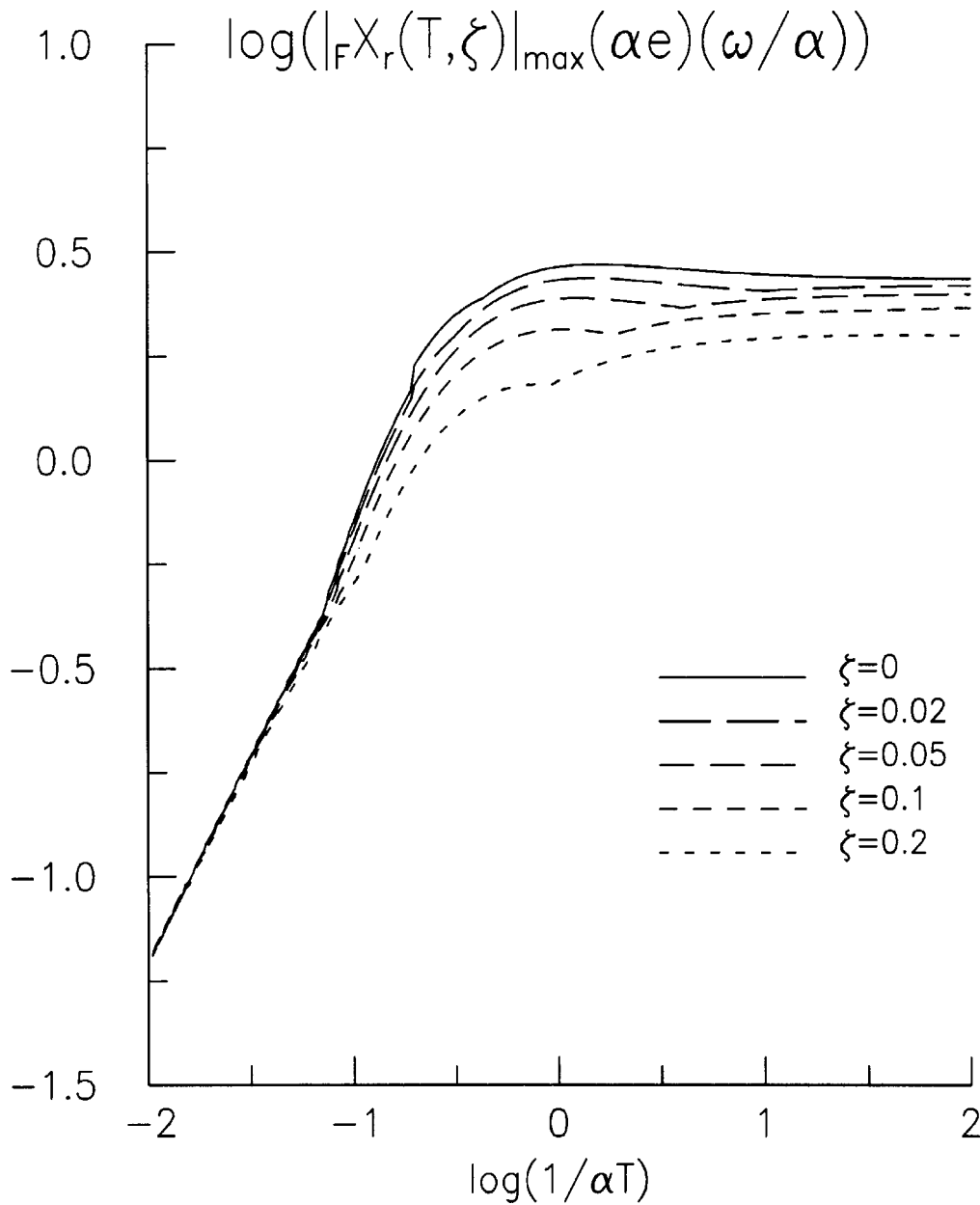
Fig. 13 Normalized amplitudes of pseudo velocity $\left| {}_F X_r(T,\zeta) \right|_{\max} \alpha e \left(\dfrac{\omega}{\alpha T} \right)$, versus dimensionless frequency $1/\alpha T$ for $\zeta = 0, 0.02, 0.05, 0.1$ and 0.2 (the ground displacement, $d_F(t)$, is the far-field pulse, with corner frequency α)

$$d_F(t) \sim d_{F,\max} \, \alpha e \, t e^{-\alpha t} \tag{26}$$

The actual ground motion is more complicated and cannot be described in detail by Equation (26); but the advantage of using this equation is that $d_F(t)$ can be related in a simple and direct way to the basic parameters governing the earthquake source.

Figure 13 shows the logarithm of the normalized (for peak value of the ground displacement $d_F(t)$ equal to one) pseudo relative velocity spectrum PSV. In terms of the dimensionless variables, PSV is equal to $\left| {}_F X_r(T,\zeta) \right|_{\max} (\alpha e)(\omega/\alpha)$. It is plotted versus $\log_{10} \dfrac{1}{\alpha T}$, for five damping values, $\zeta = 0.0$, 0.02, 0.05, 0.1 and 0.2. For $\alpha T > 2.34$, the PSV spectra diminish like $1/(\alpha T)$. For $\alpha T < 2.34$, the PSV amplitudes are essentially constant.

To extend the Pseudo Relative Velocity Spectrum $\mathrm{PSV}(T)$, described by Equation (25), beyond the period T_c, we use the functional form of $\left|_F X_r(T,\zeta)\right|_{max}(e\omega)$, and scale it by $d_{F,max}$ such that at T_c

$$\left|_F X_r(T_c,\zeta)\right|_{max} \frac{2\pi e}{T_c} d_{F,max} = \mathrm{PSV}(T_c) \tag{27}$$

Then,

$$d_{F,max} = \frac{T_c}{2\pi e} \frac{\mathrm{PSV}(T_c)}{\left|_F X_r(T_c,\zeta)\right|_{max}} \tag{28}$$

2.2 Near-Field Extension

To find $\left|_N X_r(T,\zeta)\right|_{max}$, which can represent the long period PSV spectral amplitudes in the near-field for $T > T_c$, Trifunac (1995a) considers

$$d_N(t) = d_{N,max}\left(1 - e^{-t/\tau}\right) \tag{29}$$

Here, $d_{N,max}$ represents the static permanent displacement at a station caused by an earthquake, t is time, and τ is the characteristic time. The details of actual ground motion are more complicated, but, for very long period oscillators, Equation (29) should give approximate estimates of the relative response.

Figure 14 shows the normalized (for $d_{N,max} = 1$) spectra $\mathrm{PSV} \equiv \left|_N X_r(T,\zeta)\right|_{max}(\omega\tau)$, plotted versus $\log_{10}\left(\frac{\tau}{T}\right)$. For $\frac{\tau}{T} < 0.2$, the PSV spectra for near-field displacement diminish like $\frac{\tau}{T}$. For $\frac{\tau}{T} > 0.2$, the PSV amplitudes are essentially constant.

To extend the PSV amplitudes to $T > T_c$, Trifunac (1995a) writes

$$\frac{2\pi\tau}{T_c} \left|_N X_r(T_c,\zeta)\right|_{max} d_{N,max} = \mathrm{PSV}(T_c) \tag{30}$$

and

$$d_{N,max} = \frac{\mathrm{PSV}(T_c)}{\left|_N X_r(T_c,\zeta)\right|_{max}} \frac{T_c}{2\pi\tau} \tag{31}$$

Here, $d_{N,max}$ represents an estimate of the permanent ground displacement at the site, where $\mathrm{PSV}(T_c)$ has been computed.

2.3 Transition between Near-Field and Far-Field Spectra

To provide a continuous transition between $\mathrm{PSV}_{NF}(T) \equiv \left|_N X_r(T,\zeta)\right|_{max} \frac{2\pi}{T}\tau d_{N,max}$ and $\mathrm{PSV}_{FF}(T) \equiv \left|_F X_r(T,\zeta)\right|_{max} e\frac{2\pi}{T} d_{F,max}$, and to complete a representation for use in engineering applications, Trifunac (1995a) uses the results of Jovanovich et al. (1974). They showed that the error in approximating the static displacement field following an earthquake by a point source is typically less than 5 percent at distances greater than $4L$, where L is the source length. We define the distance S_1, between the station and the "top" of the vertical fault with "dimension" S and at depth H, as

$$S_1 = \begin{cases} \left[R^2 + (H-S)^2\right]^{1/2}, & H \geq S \\ R, & H < S \end{cases} \tag{32}$$

Here, $S = 0.01 \times 10^{.5M}$, when $S \leq 30$ km, $S = 30$ km for larger events, and then, $\mathrm{PSV}_{NF}(T)$ and $\mathrm{PSV}_{FF}(T)$ can be combined as follows:

$$\mathrm{PSV}(T) = \mathrm{PSV}_{NF}(T)e^{-\left(\frac{3S_1}{4S}\right)} + \mathrm{PSV}_{FF}(T)\left(1 - e^{-\left(\frac{3S_1}{4S}\right)}\right), \quad T > T_c \tag{33}$$

In the above, $3/4$ is used to scale S_1/S, so that when $S_1/S = 4$, the exponent is equal to 3, $\left(e^{-3} \sim 0.05\right)$. For $T < T_c$, equations of the type of Equation (25) apply (Lee, 1989, 1990, 1991, 1993).

For $f < f_{co}\left(= 1/T_c\right)$, the heavy solid lines in Figure 12 show $\mathrm{PSV}(T)$ computed from Equation (33). For $R = 10$ km, $H = 5$ km, and $M = 4$ (bottom heavy solid line), since S_1 and Δ are both greater than $4S$, $\mathrm{PSV}_{FF}(T)$ contributes mainly to $\mathrm{PSV}(T)$, and so, $\mathrm{PSV}(T) \sim 1/T$. For $M \geq 7$, S_1 and Δ are smaller than $4S$, and the amplitudes of $\mathrm{PSV}(T)$ shown in Figure 12 are dominated by the flat portion of $\left|_N X_r(T,\zeta)\right|_{\max} e \dfrac{2\pi}{T} d_{N,\max}$ (see Figure 14), for T near and shorter than $\sim 5\tau$. For $M = 5$ and 6, the spectra, $\mathrm{PSV}(T)$, display progressively changing slope for $f < 1/\tau$. With increasing M (increasing S), this slope decreases from -1 towards 0, as M goes from 4 to 7, in the period (frequency) range shown in Figure 12.
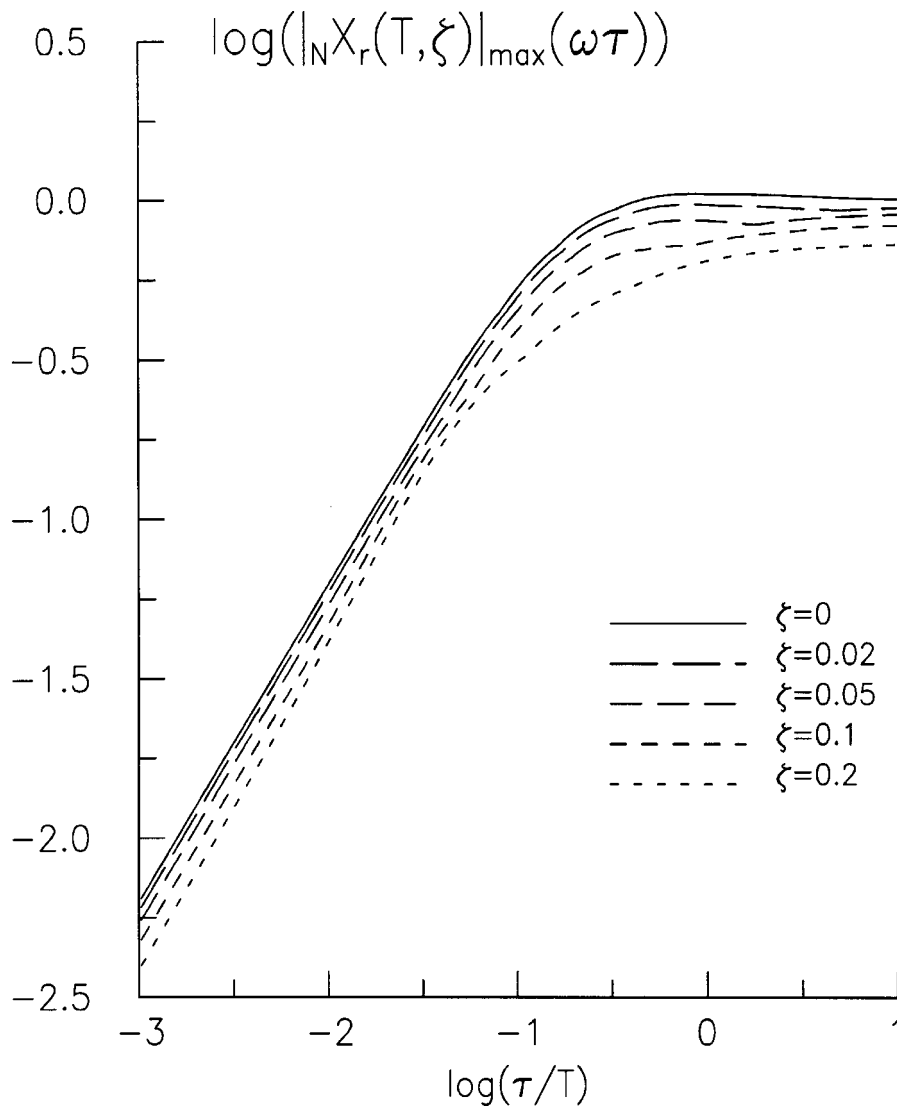
Fig. 14 $\left|_N X_r(T,\zeta)\right|_{\max}(\omega\tau)$, normalized PSV spectra versus dimensionless frequency $\dfrac{\tau}{T}$ for $\zeta = 0, 0.02, 0.05, 0.1$ and 0.2 (τ is the characteristic source time, and the displacement, $d_N(t)$, is the near-field displacement)
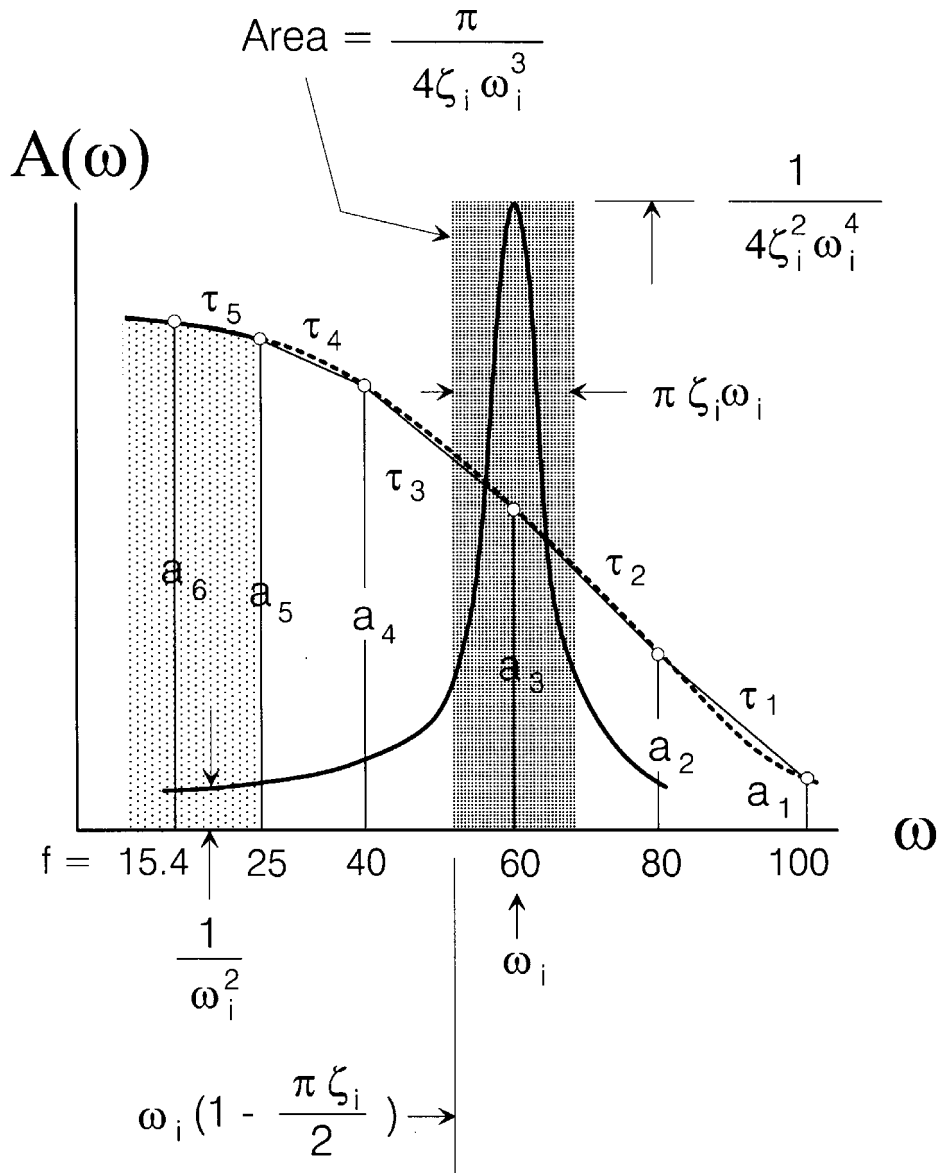
Fig. 15   Fourier amplitude spectra of strong motion acceleration $A(\omega)$ with amplitudes $a_5, a_4, ... a_1$ at $f = 25, 40, 60, 80$ and 100 Hz (the mean square interval is shown by shaded rectangle; estimates of τ_Q in the respective frequency intervals are shown by τ_1 through τ_4 (from Trifunac (1995b))

3.   Short Period Extension

To extrapolate the $\mathrm{PSV}(T)$ spectral amplitudes to periods shorter than $1/25$ s, it is necessary to employ the properties of the Fourier amplitude spectra at high frequencies (Trifunac, 1994a, 1994b). Then, using expressions for the expected values of the peaks of a random function, which is characterized by a narrow (peaked) transfer function, it is possible to derive the functional form for the extrapolation equations.

3.1 Fourier Amplitude Spectra of Strong Motion Acceleration at High Frequencies

In the real earth, noticeable attenuation takes place for frequencies higher than 1 to 10 Hz, and may be described empirically by $e^{-\pi\tau_Q f}$, where $\tau_Q = \Delta/(Q\beta)$ (Δ is the distance travelled by the wave, β is the velocity of shear waves, and Q is the attenuation quality factor).

From average travel times in Southern California, for short distances, the average shear wave velocity can be approximated by $\beta \sim 3.35 + .00175\,\Delta$, and then, Q can be computed from τ_Q versus frequency. The results show Q increasing proportionally with f for $f > 20$ Hz. For $\Delta < 100$ km and for $f > 20$ Hz, the average Q can be approximated by (Trifunac, 1994b)

$$Q \approx \left(0.367\Delta - 0.0014\Delta^2\right)f \tag{34}$$

Also,

$$\tau_Q \approx \frac{1}{\left(1.23 - 0.00405\Delta\right)f} \tag{35}$$

3.2 Extrapolation Equations

Trifunac (1995b) uses the results of Rice (1944, 1945) and of Cartwright and Longuet-Higgins (1956) for a functional relationship between the expected peak amplitudes of random functions and of their characterization in terms of their root-mean-square amplitude, r_{rms}, and the width, ε, of their energy spectrum. For a time-segment containing N peaks, the expected peak amplitude of response function $r(t)$, r_{max}, can be approximated by

$$E\left[r_{\text{max}}\right] \approx \bar{r}\left[\ln\left(1 - \varepsilon^2\right)^{1/2} N\right]^{1/2} \tag{36}$$

where, $\bar{r}$ is the root mean square amplitude of all the peaks of $r(t)$. For intermediate and small ε, it can be shown that $\bar{r} \sim \sqrt{2}r_{\text{rms}}$, where r_{rms} is the root-mean-square value of $r(t)$. To extrapolate the response spectrum amplitudes from $\text{SD}\left(T = \frac{1}{25}\right)$ to $\text{SD}(T)$ for $25 < \frac{1}{T} < 100$ Hz, Trifunac (1995b) writes

$$\rho_{2,1} = \frac{E\left[{}_2 r_{\text{max}}\right]}{E\left[{}_1 r_{\text{max}}\right]} \tag{37}$$

$$\rho_{2,1} \approx \frac{\bar{r}_2\left[\ln\left(1 - \varepsilon_2^2\right)^{1/2} N_2\right]^{1/2}}{\bar{r}_1\left[\ln\left(1 - \varepsilon_1^2\right)^{1/2} N_1\right]^{1/2}} \tag{38}$$

where, the subscripts 1 and 2 refer to $r_1(t)$ and $r_2(t)$, evaluated for two different oscillator frequencies, f_1 and f_2.

Assuming that ε does not change significantly, as the frequency f changes from f_1 to f_2, this suggests that $\ln\left(1 - \varepsilon_1^2\right)^{1/2} N_1 \sim \ln\left(1 - \varepsilon_2^2\right)^{1/2} N_2$, and so,

$$\rho_{2,1} \approx \bar{r}_2 / \bar{r}_1 \tag{39}$$

Using the mean square approximation (Figure 15), this can be evaluated numerically,

$$\rho_{i+1,i}^2 \approx \frac{\dfrac{1}{\omega_{i+1}^4}\displaystyle\int_0^{\omega_{i+1} - \zeta_{i+1}\omega_{i+1}\pi/2}\left|A(\omega)\right|^2 d\omega + \dfrac{a_k^2\pi}{4\zeta_{i+1}\omega_{i+1}^3}}{\dfrac{1}{\omega_i^4}\displaystyle\int_0^{\omega_i - \zeta_i\omega_i\pi/2}\left|A(\omega)\right|^2 d\omega + \dfrac{a_{k+1}^2\pi}{4\zeta_i\omega_i^3}} \tag{40}$$

where, a_k amplitudes are as denoted in Figure 15.

Since $\text{PSV}(T) = \dfrac{2\pi}{T}\,\text{SD}(T)$,

$$\text{PSV}(T_{i+1}) \approx \text{PSV}(T_i)\frac{T_i}{T_{i+1}}\rho_{i+1,i} \tag{41}$$

where, $T_i = 1/f_i$. In Equation (40), the term, $\pi a_k^2 / (4\zeta_i \omega_i^3)$, dominates for $f \leq 10 - 20$ Hz. For higher frequencies, as $f \to \infty$, this term becomes negligible, and $\rho_{i+1,i} \to 1$ (Figure 16).
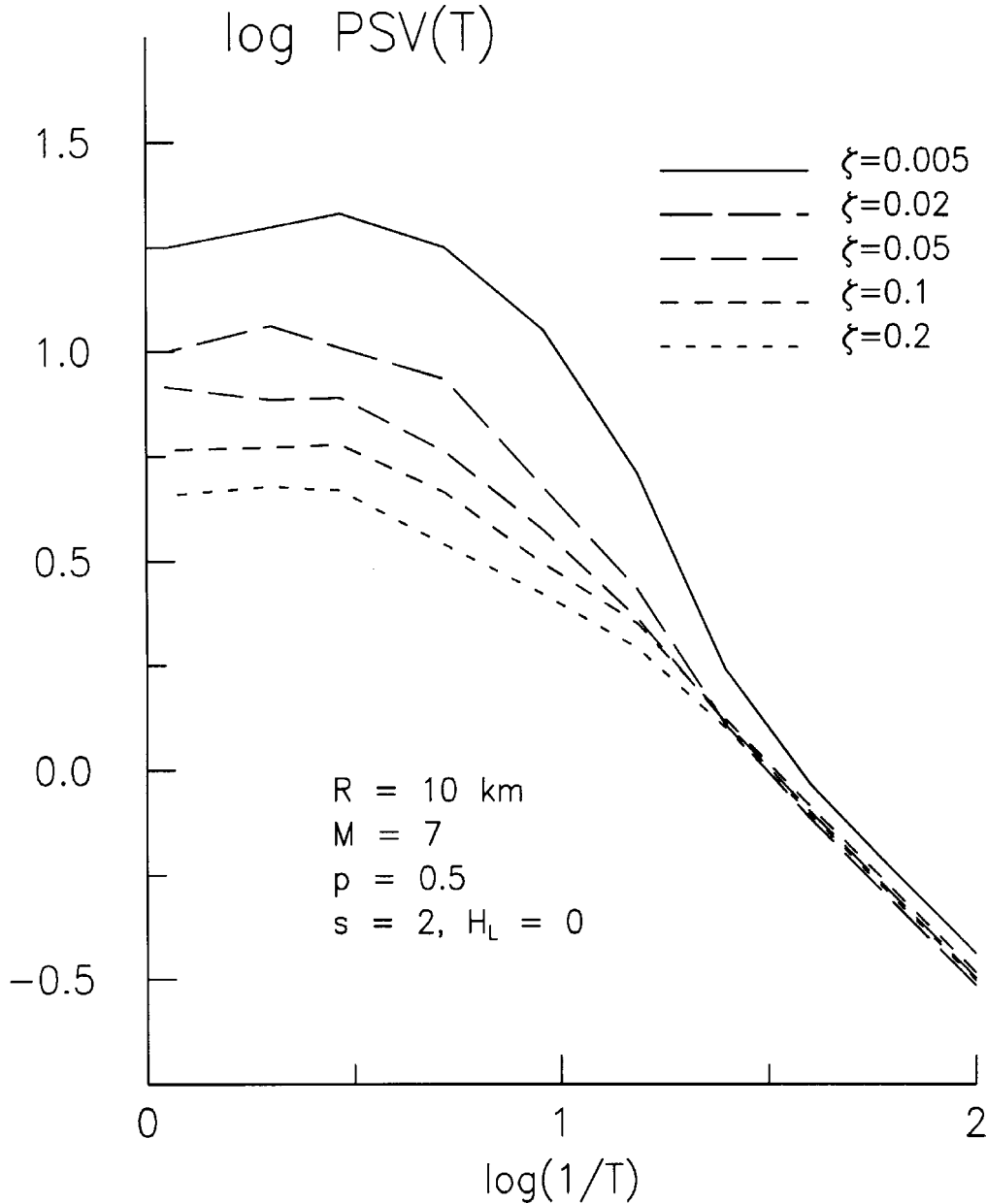
Fig. 16 An example of using Equation (41) to extrapolate response spectra $\text{PSV}(T)$ to periods $T < 1/25$ s

4. DISCUSSION

The largest uncertainties are believed to exist near T_c, where the empirical scaling models approach the recording and processing noise. The tests performed so far suggest that the resulting $\text{PSV}(T)$ are very realistic for $3.5 < M < 7$ and for horizontal ground motion. The slopes and amplitudes of empirically computed $\text{FS}(T)$ (Trifunac, 1993a, 1993b) and $\text{PSV}(T)$ for vertical motions suggest that near $T = T_c$, our empirical models may not be reliable for $M > 6.5$. To understand these amplitudes, we

need more recorded accelerograms for $M > 7$, and so, we must patiently wait for this data to become available.

Extrapolation of $\text{PSV}(T)$ by Equation (33) from T_c towards $T \to \infty$ agrees favorably with the known trends of seismic moment M_o, peak ground displacements, and of the average dislocation amplitudes, $\overline{u}$, versus earthquake magnitude. Since the corner frequency in Fourier spectrum amplitudes, $1/\tau$, in the near-field ground motion is $\sim v/r$, where v is the dislocation velocity (typically between 2 and 3 km/s), and r is the representative source dimension, it is seen that τ can be larger than T_c. This is so, assuming that, for the frequencies considered here, the rupture occurs as a "smooth" process. Many studies have suggested that the faults slip irregularly, with large dislocations distributed at several or at many "hot" spots with large dislocation amplitudes, thus making larger events look like a sequence of smaller events. While this faulting behavior can affect τ appreciably, we do not have at present, reliable data to introduce and to verify such behavior.

The highly "local" nature of strong motion recording, local in the sense of the proximity to the fault (often less than, say 50 km), and the fact that it is $\overline{u}$ and not the overall source magnitude or moment and long source dimensions (L) that govern the near-field strong motion amplitudes, all agree with the observed trends of strong motion amplitudes predicted by the above outlined approach.

REFERENCES

1. Alford, J.L., Housner, G.W. and Martel, R.R. (1951). "Spectrum Analysis of Strong-Motion Earthquakes", Earthquake Eng. Res. Lab., Calif. Inst. of Tech., Pasadena, U.S.A.

2. Amini, A. and Trifunac, M.D. (1985). "Statistical Extension of Response Spectrum Superposition", Int. J. Soil Dynam. Earthquake Engg., Vol. 4, No. 2, pp. 54-63.

3. Benioff, H. (1934). "The Physical Evaluation of Seismic Destructiveness", Bull. Seism. Soc. Amer., Vol. 24, pp. 398-403.

4. Biot, M.A. (1932). "Vibrations of Building during Earthquake", Chapter II in Ph.D. Thesis No. 259 entitled "Transient Oscillations in Elastic System", Aeronautics Department, Calif. Inst. of Tech., Pasadena, California, U.S.A.

5. Biot, M.S. (1933). "Theory of Elastic Systems Vibrating under Transient Impulse with an Application to Earthquake-Proof Buildings", Proc. National Academy of Sciences, Vol. 19, No. 2, pp. 262-268.

6. Biot, M.A. (1934). "Theory of Vibration of Building during Earthquake", Zeitschrift *für* Angewandte Matematik und Mechanik, Vol. 14, No. 4, pp. 213-223.

7. Biot, M.A. (1941). "A Mechanical Analyzer for the Prediction of Earthquake Stresses", Bull. Seism. Soc. Amer., Vol. 31, pp. 151-171.

8. Biot, M.A. (1942). "Analytical and Experimental Methods in Engineering Seismology", ASCE Transactions, Vol. 108, pp. 365-408.

9. Borcherdt, R. and Gibbs, J.F. (1976). "Effects of Local Geological Conditions in the San Francisco Bay Region on Ground Motions and Intensities of the 1906 Earthquake", Bull. Seism. Soc. Amer., Vol. 66, pp. 467-500.

10. Cartwright, D.E. and Longuet-Higgins, M.S. (1956). "The Statistical Distribution of Maxima of a Random Function", Proc. Royal Soc. London, Ser. A327, pp. 212-232.

11. Duke, C.M. (1958). "Bibliography of Effects of Soil Conditions on Earthquake Damage", Earthquake Engg. Res. Inst.

12. Gutenberg, B. (1957). "Effects of Ground on Earthquake Motion", Bull. Seism. Soc. Amer., Vol. 47, pp. 221-250.

13. Gupta, I.D. and Trifunac, M.D. (1988a). "Order Statistics of Peaks in Earthquake Response", ASCE J. Engng Mech., Vol. 114, No. 10, pp. 1605-1627.

14. Gupta, I.D. and Trifunac, M.D. (1988b). "Attenuation of Intensity with Epicentral Distance in India", Int. J. Soil Dynamics and Earthquake Eng., Vol. 7, pp. 162-169.

15. Gupta, I.D. and Trifunac, M.D. (1990a). "Probabilistic Spectrum Superposition for Response Analysis Including the Effects of Soil-Structure Interaction", J. Prob. Engg. Mech., Vol. 5, No. 1, pp. 9-18.

16. Gupta, V.K. and Trifunac, M.D. (1990b). "Response of Multistoried Buildings to Ground Translation and Rocking during Earthquakes", J. Prob. Engg. Mech., Vol. 5, No. 3, pp. 138-145.

17. Gupta, V.K. and Trifunac, M.D. (1991a). "Seismic Response of Multistoried Buildings Including the Effects of Soil-Structure Interaction", Soil Dynam. and Earthquake Engg., Vol. 10, No. 8, pp. 414-422.

18. Gupta, V.K. and Trifunac, M.D. (1991b). "Effects of Ground Rocking on Dynamic Response of Multistoried Buildings during Earthquakes", Structural Engg./Earthquake Engg., JSCE, Vol. 8, No. 2, pp. 43-50.

19. Housner, G.W. (1970). "Design Spectrum", Chapter 5 in "Earthquake Engineering (edited by R.L. Wiegel)", Prentice-Hall.

20. Hudson, D.E., Trifunac, M.D. and Brady, A.G. (1972). "Strong-Motion Accelerograms III, Response Spectra", Report EERL 72-80, Earthqu. Engng Res. Lab., Calif. Inst. of Tech., Pasadena, U.S.A.

21. Jordanovski, L.R., Todorovska, M.I. and Trifunac, M.D. (1993). "Total Loss in a Building Exposed to Earthquake Hazard, Part I: The Model; Part II: A Hypothetical Example", Europ. Earthqu. Engng, Vol. VI, No. 3, pp. 14-32.

22. Jovanovich, D., Husseini, M.I. and Chinnery, M.A. (1974). "Elastic Dislocations in a Layered Half Space - I. Basic Theory and Numerical Methods; II. The Point Source", Geoph. J. Royal Astr. Soc., Vol. 39, pp. 205-239.

23. Lee, V.W. (1989). "Empirical Scaling of Pseudo Relative Velocity Spectra of Recorded Strong Earthquake Motion in Terms of Magnitude and Both Local Soil and Geologic Site Classifications", Earthqu. Engng and Engng Vib., Vol. 9, No. 3, pp. 9-29.

24. Lee, V.W. (1990). "Scaling PSV Spectra in Terms of Site Intensity, and Both Local Soil and Geological Site Classifications", Europ. Earthqu. Engng, Vol. IV, No. 1, pp. 3-12.

25. Lee, V.W. (1991). "Correlation of Pseudo Relative Velocity Spectra with Site Intensity, Local Soil Classification and Depth of Sediments", Soil Dynam. Earthqu. Engng., Vol. 10, No. 3, pp. 141-151.

26. Lee, V.W. (1993). "Scaling PSV from Earthquake Magnitude, Local Soil and Geological Depth of Sediments", ASCE J. Geotech. Engng, Vol. 119, No. 1, pp. 108-126.

27. Lee, V.W. and Trifunac, M.D. (1985). "Attenuation of Modified Mercalli Intensity for Small Epicentral Distance in California", Report CE 85-01, Dept. of Civil Eng., Univ. of Southern California, Los Angeles, California, U.S.A.

28. Lee, V.W. and Trifunac, M.D. (1993). "Empirical Scaling of Fourier Amplitude Spectra in Former Yugoslavia", Europ. Earthqu. Engng, Vol. VII, No. 2, pp. 47-61.

29. Lee, V.W. and Trifunac, M.D. (1995a). "Frequency Dependent Attenuation Function and Fourier Amplitude Spectra of Strong Earthquake Ground Motion in California", Report CE 95-03, Dept. of Civil Eng., Univ. of Southern California, Los Angeles, California, U.S.A.

30. Lee, V.W. and Trifunac, M.D. (1995b). "Pseudo Relative Velocity Spectra of Strong Earthquake Ground Motion in California", Report CE 95-04, Dept. of Civil Eng., Univ. of Southern California, Los Angeles, California, U.S.A.

31. Lee, V.W., Trifunac, M.D., Todorovska, M.I. and Novikova, E.I. (1995). "Empirical Equations Describing Attenuation of the Peaks of Strong Ground Motion, in Terms of Magnitude, Distance, Path Effects, and Site Conditions", Report CE 95-02, Dept. of Civil Eng., Univ. of Southern California, Los Angeles, California, U.S.A.

32. Newmark, N.M., Degenkolb, H.J., Chopra, A.K., Veletsos, A.S., Rosenblueth, E. and Sharpe, R.L. (1977). "Seismic Design and Analysis Provisions for the United States", Proc. Sixth World Conf. Earthqu. Engng, New Delhi, Vol. II, pp. 1986-1991.

33. Novikova, E.I. and Trifunac, M.D. (1995). "Frequency Dependent Duration of Strong Earthquake Ground Motion: Updated Empirical Equations", Report CE 95-01, Dept. of Civil Eng., Univ. Southern California, Los Angeles, California, U.S.A.

34. Rice, S.O. (1944). "Mathematical Analysis of Random Noise", Bell System Tech. J., Vol. 23, pp. 282-332.

35. Rice, S.O. (1945). "Mathematical Analysis of Random Noise", Bell System Tech. J., Vol. 24, pp. 46-156.

36. Richter, C.F. (1958). "Elementary Seismology", Freeman and Co., San Francisco.

37. Seed, H.B., Ugas, C. and Lysmer, J. (1974). "Site Dependent Spectra for Earthquake Resistant Design", Report EERC 74-12, Earthqu. Engng Res. Center, U.C. Berkeley, U.S.A.

38. Todorovska, M.I. (1994a). "A Note on Distribution of Amplitudes of Peaks in Structural Response including Uncertainties of the Exciting Ground Motion and of the Structural Model", Soil Dynam. Earthqu. Engng, Vol. 14, No. 3, pp. 211-217.

39. Todorovska, M.I. (1994b). "Order Statistics of Functionals of Strong Motion", Soil Dynam. Earthqu. Engng, Vol. 13, No. 3, pp. 149-161.

40. Todorovska, M.I. (1994c). "Comparison of Response Spectrum Amplitudes from Earthquakes with Lognormally and Exponentially Distributed Return Period", Soil Dynam. Earthqu. Engng., Vol. 13, No. 1, pp. 97-116.

41. Trifunac, M.D. (1973). "Analysis of Strong Earthquake Ground Motion for Prediction of Response Spectra", Int. J. Earthqu. Engng Struct. Dynam., Vol. 2, No. 1, pp. 59-69.

42. Trifunac, M.D. (1976a). "Preliminary Analysis of the Peaks of Strong Earthquake Ground Motion - Dependence of Peaks on Earthquake Magnitude, Epicentral Distance and Recording Site Conditions", Bull. Seism. Soc. Amer., Vol. 66, pp. 189-219.

43. Trifunac, M.D. (1976b). "Preliminary Empirical Model for Scaling Fourier Amplitude Spectra of Strong Ground Acceleration in Terms of Earthquake Magnitude, Source to Station Distance and Recording Site Conditions", Bull. Seism. Soc. Amer., Vol. 68, pp. 1345-1373.

44. Trifunac, M.D. (1976c). "A Note on the Range of Peak Amplitudes of Recorded Accelerations, Velocities and Displacements with Respect to the Modified Mercalli Intensity", Earthquake Notes, Vol. 47, No. 1, pp. 9-24.

45. Trifunac, M.D. (1977a). "Statistical Analysis of the Computed Response of Structural Response Recorders (S.R.R.) for Accelerograms Recorded in the United States of America", Sixth World Conference Earthquake Engineering, New Delhi, Vol. III, pp. 2956-2961.

46. Trifunac, M.D. (1977b). "Forecasting the Spectral Amplitudes of Strong Earthquake Ground Motion", Sixth World Conference Earthquake Engineering, New Delhi, Vol. I, pp. 139-152.

47. Trifunac, M.D. (1977c). "An Instrumental Comparison of the Modified Mercalli (M.M.I.) and Medvedev-Karnik-Sponheuer (M.K.S.) Intensity Scales", Sixth World Conference Earthquake Engineering, New Delhi, Vol. I, pp. 715-721.

48. Trifunac, M.D. (1977d). "Uniformly Processed Strong Earthquake Ground Accelerations in the Western United States of America for the Period from 1933 to 1971; Pseudo Relative Velocity Spectra and Processing Noise", Report CE 77-04, Dept. of Civil Eng., Univ. of Southern California, Los Angeles, California, U.S.A.

49. Trifunac, M.D. (1978). "Response Spectra of Earthquake Ground Motion", ASCE J. Eng. Mech., Vol. 104, No. EM5, pp. 1081-1097.

50. Trifunac, M.D. (1979). "Preliminary Empirical Model for Scaling Fourier Amplitude Spectra of Strong Motion Acceleration in Terms of Modified Mercalli Intensity and Geologic Site Conditions", Int. J. Earthqu. Engng and Struct. Dynam., Vol. 7, pp. 63-74.

51. Trifunac, M.D. (1988). "Seismic Microzonation Mapping via Uniform Risk Spectra", Proc. 9th World Conf. Earthqu. Engng, Tokyo-Kyoto, Japan, Vol. VII, pp. 75-80.

52. Trifunac, M.D. (1989a). "Dependence of Fourier Spectrum Amplitudes of Recorded Strong Earthquake Accelerations on Magnitude, Local Soil Conditions and on Depth of Sediments", Int. J. Earthquake Eng. Structural Dyn., Vol. 18, No. 7, pp. 999-1016.

53. Trifunac, M.D. (1989b). "Empirical Scaling of Fourier Spectrum Amplitudes of Recorded Strong Earthquake Accelerations in Terms of Magnitude and Local Soil and Geologic Site Conditions", Earthquake Eng. Eng. Vibration, Vol. 9, No. 2, pp. 23-44.

54. Trifunac, M.D. (1989c). "Scaling Strong Motion Fourier Spectra by Modified Mercalli Intensity, Local Soil and Geologic Site Conditions", Structural Eng./Earthquake Eng., JSCE, Vol. 6, No. 2, pp. 217-224.

55. Trifunac, M.D. (1989d). "Threshold Magnitudes Which Exceed the Expected Ground Motion during the Next 50 Years in a Metropolitan Area", Geofizika, Vol. 6, pp. 1-12.

56. Trifunac, M.D. (1990a). "How to Model Amplification of Strong Earthquake Motions by Local Soil and Geologic Site Conditions", Earthqu. Engng Struct. Dynam., Vol. 19, No. 6, pp. 833-846.

57. Trifunac, M.D. (1990b). "A Microzonation Method Based on Uniform Risk Spectra", Soil Dynam. Earthqu. Engng, Vol. 9, No. 1, pp. 34-43.

58. Trifunac, M.D. (1991a). "Empirical Scaling of Fourier Spectrum Amplitudes of Recorded Strong Earthquake Accelerations in Terms of Modified Mercalli Intensity, Local Soil Conditions and Depth of Sediments", Int. J. Soil Dynamics Earthquake Eng., Vol. 10, No.1, pp. 65-72.

59. Trifunac, M.D. (1991b). " M_L^{SM} ", Int. J. Soil Dynam. Earthqu. Engng, Vol. 10, No. 1, pp. 17-25.

60. Trifunac, M.D. (1993a). "Long Period Fourier Amplitude Spectra of Strong Motion Acceleration", Soil Dynam. Earthqu. Engng, Vol. 12, No. 6, pp. 363-382.

61. Trifunac, M.D. (1993b). "Broad Band Extension of Fourier Amplitude Spectra of Strong Motion Acceleration", Report CE 93-01, Dept. of Civil Eng., Univ. of Southern California, Los Angeles, California, U.S.A.

62. Trifunac, M.D. (1994a). "Fourier Amplitude Spectra of Strong Motion Acceleration: Extension to High and Low Frequencies", Earthqu. Engng Struct. Dynam., Vol. 23, No. 4, pp. 389-411.

63. Trifunac, M.D. (1994b). " Q and High Frequency Strong Motion Spectra", Soil Dynam. Earthqu. Engng, Vol. 13, No. 4, pp. 149-161.

64. Trifunac, M.D. (1994c). "Earthquake Source Variables for Scaling Spectral and Temporal Characteristics of Strong Ground Motion", Proc. 10th Europ. Conf. Earthqu. Eng., Vienna, Austria, Vol. 4, pp. 2585-2590.

65. Trifunac, M.D. (1994d). "Response Spectra of Strong Motion Acceleration: Extension to High and Low Frequencies", Proc. 10th Europ. Conf. Earthqu. Eng., Vienna, Austria. Vol. 1, pp. 203-208.

66. Trifunac, M.D. (1994e). "Broad Band Extension of Pseudo Relative Velocity Spectra of Strong Motion", Report CE 94-02, Dept. of Civil Eng., Univ. Southern California, Los Angeles, California, U.S.A.

67. Trifunac, M.D. (1995a). "Pseudo Relative Velocity Spectra of Earthquake Ground Motion at Long Periods", Soil Dynam. Earthqu. Engng, Vol. 14, No. 5, pp. 331-346.

68. Trifunac, M.D. (1995b). "Pseudo Relative Velocity Spectra of Earthquake Ground Motion at High Frequencies", Earthqu. Engng Struct. Dynam., Vol. 24, No. 8, pp. 1113-1130.

69. Trifunac, M.D. and Anderson, J.G. (1977). "Preliminary Empirical Models for Scaling Absolute Acceleration Spectra", Report CE 77-03, Dept. of Civil Eng., Univ. of Southern California, Los Angeles, California, U.S.A.

70. Trifunac, M.D. and Anderson, J.G. (1978a). "Preliminary Empirical Models for Scaling Pseudo Relative Velocity Spectra", Report CE 78-04, Dept. of Civil Eng., Univ. of Southern California, Los Angeles, California, U.S.A.

71. Trifunac, M.D. and Anderson, J.G. (1978b). "Preliminary Models for Scaling Relative Velocity Spectra", Report CE 78-05, Dept. of Civil Eng., Univ. of Southern California, Los Angeles, California, U.S.A.

72. Trifunac, M.D. and Anderson, J.C. (1978c). "Estimation of Relative Velocity Spectra", Proc. 6th Symp. Earthquake Engineering, University of Roorkee, India.

73. Trifunac, M.D. and Brady, A.G. (1975a). "A Study on the Duration of Strong Earthquake Ground Motion", Bull. Seism. Soc. Amer., Vol. 65, pp. 581-626.

74. Trifunac, M.D. and Brady, A.G (1975b). "On the Correlation of Seismic Intensity Scales with the Peaks of Recorded Strong Ground Motion", Bull. Seism. Soc. Amer., Vol. 65, pp. 139-162.

75. Trifunac, M.D. and Brady, A.G. (1975c). "On the Correlation of Seismoscope Response with Earthquake Magnitude and Modified Mercalli Intensity", Bull. Seism. Soc. Amer., Vol. 65, pp. 307-321.

76. Trifunac, M.D. and Brady, A.G. (1975d). "Correlations of Peak Acceleration, Velocity and Displacement with Earthquake Magnitude, Epicentral Distance and Site Conditions", Int. J. Earthquake Engineering Struct. Dynamics, Vol. 4, pp. 455-471.

77. Trifunac, M.D. and Brady, A.G. (1975e). "On the Correlation of Peak Accelerations of Strong-Motion with Earthquake Magnitude, Epicentral Distance and Site Conditions" Proc. U.S. National Conference Earthquake Engineering, Ann Arbor, Michigan, U.S.A., pp. 43-52.

78. Trifunac, M.D. and Gupta, V.K. (1991). "Pseudo Relative Acceleration Spectrum", ASCE J. Engineering Mech., Vol. 117, No. 4, pp. 924-927.

79. Trifunac, M.D. and Lee, V.W. (1978). "Dependence of Fourier Amplitude Spectra of Strong Motion Acceleration on the Depth of Sedimentary Deposits", Report CE 78-14, Dept. of Civil Eng., Univ. of Southern California, Los Angeles, California, U.S.A.

80. Trifunac, M.D. and Lee, V.W. (1979). "Dependence of Pseudo Relative Velocity Spectra of Strong Motion Acceleration on the Depth of Sedimentary Deposits", Report CE 79-02, Dept. of Civil Eng., Univ. of Southern California, Los Angeles, California, U.S.A.

81. Trifunac, M.D. and Lee, V.W. (1980). "Fourier Amplitude Spectra of Strong Motion Acceleration", Bulletin EAEE, Vol. 6, pp. 2-18.

82. Trifunac, M.D. and Lee, V.W. (1985a). "Frequency Dependent Attenuation of Strong Earthquake Ground Motion", Report CE 85-02, Dept. of Civil Eng., Univ. of Southern California, Los Angeles, California, U.S.A.

83. Trifunac, M.D. and Lee, V.W. (1985b). "Preliminary Empirical Model for Scaling Fourier Amplitude Spectra of Strong Ground Acceleration in Terms of Earthquake Magnitude, Source to Station Distance, Site Intensity and Recording site Conditions", Report CE 85-03, Dept. of Civil Eng., Univ. of Southern California, Los Angeles, California, U.S.A.

84. Trifunac, M.D and Lee, V.W. (1985c). "Preliminary Empirical Model for Scaling Pseudo Relative Velocity Spectra of Strong Earthquake Acceleration in Terms of Magnitude, Distance, Site Intensity and Recording Site Conditions", Report CE 85-04, Dept. of Civil Eng., Univ. of Southern California, Los Angeles, California, U.S.A.

85. Trifunac, M.D. and Lee, V.W. (1987). "Direct Empirical Scaling of Response Spectral Amplitudes from Various Site and Earthquake Parameters", Report NUREG/CE-4903, U.S. Nuclear Regulatory Commission, Vol. 1.

86. Trifunac, M.D. and Lee, V.W. (1989a). "Empirical Models for Scaling Fourier Amplitude Spectra of Strong Ground Acceleration in Terms of Earthquake Magnitude, Source to Station Distance, Site Intensity and Recording Site Conditions", Int. J. Soil Dynamics Earthquake Eng., Vol. 8, No. 3, pp. 110-125.

87. Trifunac, M.D. and Lee, V.W. (1989b). "Empirical Models for Scaling Pseudo Relative Velocity Spectra of Strong Earthquake Accelerations in Terms of Magnitude, Distance, Site Intensity and Recording Site Conditions", Int. J. Soil Dynamics Earthquake Eng., Vol. 8, No. 3, pp. 126-144.

88. Trifunac, M.D. and Lee, V.W. (1990). "Frequency Dependent Attenuation of Strong Earthquake Ground Motion", Int. J. Soil Dynam. Earthqu. Engng, Vol. 9, No. 1, pp. 3-15.

89. Trifunac, M.D. and Lee, V.W. (1992). "A Note on Scaling Peak Acceleration, Velocity and Displacement of Strong Earthquake Shaking by Modified Mercalli Intensity (MMI) and Site Soil and Geologic Conditions", Soil Dynamics Earthquake Eng., Vol. 11, No. 2, pp. 101-110.

90. Trifunac, M.D. and Novikova, E.I. (1994). "State of the Art Review of Strong Motion Duration", Proc. 10th Europ. Conf. Earthqu. Eng., Vienna, Austria, Vol. 1, pp. 131-140.

91. Trifunac, M.D. and Todorovska, M.I. (1989a). "Attenuation of Seismic Intensity in Albania and Yugoslavia", Int. J. Struct. Dynamics Earthquake Eng., Vol. 10, No. 5, pp. 617-631.

92. Trifunac, M.D. and Todorovska, M.I. (1989b). "Methodology for Selection of Earthquake Design Motions for Important Engineering Structures", Report CE 89-01, Dept. of Civil Eng., Univ. Southern Calif., Los Angeles, California, U.S.A.

93. Trifunac, M.D. and Todorovska, M.I. (2001a). "A Note on the Useable Range in Accelerographs Recording Translation", Soil Dynamics Earthquake Eng., Vol. 21, No. 4, pp. 275-286.

94. Trifunac, M.D. and Todorovska, M.I. (2001b). "Evolution of Accelerographs, Data Processing, Strong Motion Arrays and Amplitude and Spatial Resolution in Recording Strong Earthquake Motion", Soil Dynamics Earthquake Eng., Vol. 21, No. 6, pp. 537-555.

95. Trifunac, M.D. and Živčić, M. (1991). "A Note on Instrumental Comparison of the Modified Mercalli Intensity (MMI) in the Western United States and the Mercalli-Cancani-Sieberg (MCS) Intensity in Yugoslavia", European Earthquake Eng., Vol. V, No. 1, pp. 2-26.

96. Trifunac, M.D., Lee, V.W., Cao, H. and Todorovska, M.I. (1988). "Attenuation of Seismic Intensity in Balkan Countries", Report CE 88-01, Dept. of Civil Eng., Univ. of Southern Calif., Los Angeles, California, U.S.A.

97. Trifunac, M.D., Lee, V.W., Živčić, M. and Manic, M. (1991). "On the Correlation of Mercalli-Cancani-Sieberg Intensity Scale in Yugoslavia with the Peaks of Recorded Strong Earthquake Ground Motion", European Earthquake Eng., Vol. V, No. 1, pp. 27-33.

98. Veletsos, A.S., Newmark, N.M. and Chelapati, C.V. (1965). "Deformation Spectra for Elastic and Elastoplastic Systems Subjected to Ground Shock and Earthquake Motions", Proc. Third World Conf. Earthqu. Engng, New Zealand, Vol. II, pp. 663-680.

99. Wong, H.L. and Trifunac, M.D. (1979). "A Comparison of the Modified Mercalli (MMI) and the Japanese Meteorological Agency (JMA) Intensity Scales", Earthquake Engineering Struct. Dynamics, Vol. 7, No. 8, pp. 75-83.